Plant Physiology Preview. Published on April 6, 2017, as DOI:10.1104/pp.16.01973

SHORT TITLE

Altered cell wall structure in *FNSII*-mutant rice

CORRESPONDING AUTHORS

Yuki Tobimatsu (ytobimatsu@rish.kyoto-u.ac.jp; +81-774-38-3626) and Clive Lo (clivelo@hku.hk; +852-2299-0337)

TITLE

Disrupting Flavone Synthase II Alters Lignin and Improves Biomass Digestibility

AUTHORS

Pui Ying Lam[1,2,*], Yuki Tobimatsu[2,*,†], Yuri Takeda[2], Shiro Suzuki[2], Masaomi Yamamura[2], Toshiaki Umezawa[2,3], Clive Lo[1,†]

[1]School of Biological Sciences, The University of Hong Kong, Pokfulam, Hong Kong, China; [2]Research Institute for Sustainable Humanosphere, Kyoto University, Gokasho, Uji, Kyoto 611-0011, Japan; [3]Research Unit for Global Sustainability Studies, Kyoto University, Gokasho, Uji, Kyoto 611-0011, Japan.

ONE SENTENCE SUMMARY

Disruption of flavone synthase II gene in rice results in an altered cell wall lignin incorporating naringenin as a novel flavonoid component and improves biomass saccharification efficiency.

FOOTNOTES

[*]P.Y.L. and Yuki T. contributed equally to this work. P.Y.L., Yuki T., Yuri T., S.S., M.Y. performed experiments. P.Y.L., Yuki T., T.U., and C.L. designed research, analyzed data, and wrote the manuscript with contributions of all the other authors.

This work was supported in part by grants from the Research Grants Council of Hong Kong, China (grant nos. 17114514 and 17123315), the Japan Society for the Promotion

of Science (Grants-in-aid for Scientific Research, KAKENHI, #16K14958 and #16H06198), the Japan Science and Technology Agency / Japan International Cooperation Agency (Science and Technology Research Partnership for Sustainable Development, SATREPS), and the Research Institute for Sustainable Humanosphere, Kyoto University (grant no. 2016-5-2-1).

†*Corresponding Authors:* Yuki Tobimatsu (ytobimatsu@rish.kyoto-u.ac.jp; +81-774-38-3626) and Clive Lo (clivelo@hku.hk; +852-2299-0337)

ABSTRACT

Lignin, a ubiquitous phenylpropanoid polymer in vascular plant cell walls, is primarily derived from oxidative couplings of monolignols (*p*-hydroxycinnamyl alcohols). It was recently discovered that a wide range of grasses, including cereals, utilize a member of flavonoid, tricin (3′,5′-dimethoxyflavone), as a natural co-monomer with monolignols for cell wall lignification. Previously, we established that cytochrome P450 93G1 is a flavone synthase II (OsFNSII) indispensable for the biosynthesis of soluble tricin-derived metabolites in rice (*Oryza sativa* L.). Here, our tricin-deficient *fnsII* mutant was further analyzed with an emphasis on its cell wall structure and properties. The mutant is similar in growth to the wild-type control plants with normal vascular morphology. Chemical and NMR structural analyses demonstrated that the mutant lignin is completely devoid of tricin, indicating that FNSII activity is essential for deposition of tricin-bound lignin in rice cell walls. The mutant also showed substantially reduced lignin content with decreased syringyl/guaiacyl lignin unit composition. Interestingly, the loss of tricin in the mutant lignin appears to be partially compensated by incorporating naringenin which is a preferred substrate of OsFNSII. The *fnsII* mutant was further revealed to have enhanced enzymatic saccharification efficiency, suggesting that cell wall recalcitrance of grass biomass may be reduced through manipulation of flavonoid monomer supply for lignification.

INTRODUCTION

Phenylpropanoids are natural phenolic compounds widespread in plants and they contribute to many aspects of plant development and responses towards biotic and abiotic stimuli. The phenylpropanoid pathway starts from L-phenylalanine and/or L-tyrosine that split(s) off from primary metabolism. Non-oxidative deaminations and successive hydroxylation and/or ligation with coenzyme A (CoA) produce *p*-coumaroyl CoA which serves as a common intermediate for many classes of phenylpropanoids (Fig. 1). Branching off from *p*-coumaroyl CoA, flavonoids and monolignols are the two major downstream metabolite classes generated separately from the pathway (Dixon et al., 2002; Vogt, 2010; Barros et al., 2016).

Flavonoids are a large class of secondary metabolites widespread in vascular plants and certain bryophytes. The structures of flavonoids are highly diverse and different classes are assigned based on the modification of the C6-C3-C6 backbone. Flavonoids display various physiological functions as antioxidants (Agati et al., 2012), phytoalexins (Koes et al., 1994; Du et al., 2010b), signaling molecules (Hassan and Mathesius, 2012), or pigments (Goto and Kondo, 1991). In monocot family Poaceae, which are the grasses including the cereals, one of the predominant forms of flavonoids is tricin, a 3′,5′-dimethoxyflavone, commonly found as *O*-linked conjugates in vegetative tissues (Zhou and Ibrahim, 2010; Dong et al., 2014; Li et al., 2016). The biosynthesis of flavonoids is achieved by a combination of the phenylpropanoid pathway and the polyketide pathway. Sequential condensation of *p*-coumaroyl CoA with three malonyl CoA is catalyzed by chalcone synthase (CHS), and followed by isomerization by chalcone isomerase (CHI) to form naringenin, a flavanone which is the precursor for the biosynthesis of all the other classes of flavonoids. To produce tricin conjugates, naringenin is converted into apigenin by flavone synthase II (FNSII), and sequential hydroxylations and *O*-methylations at the flavone B-ring furnish tricin which is then further converted into the downstream tricin derivatives (Fig. 1).

Lignin, on the other hand, is an abundant phenylpropanoid polymer derived from oxidative couplings of monolignols, i.e., *p*-hydroxycinnamyl alcohols, and is one of the major cell wall components in vascular plants. By filling up spaces between cell wall

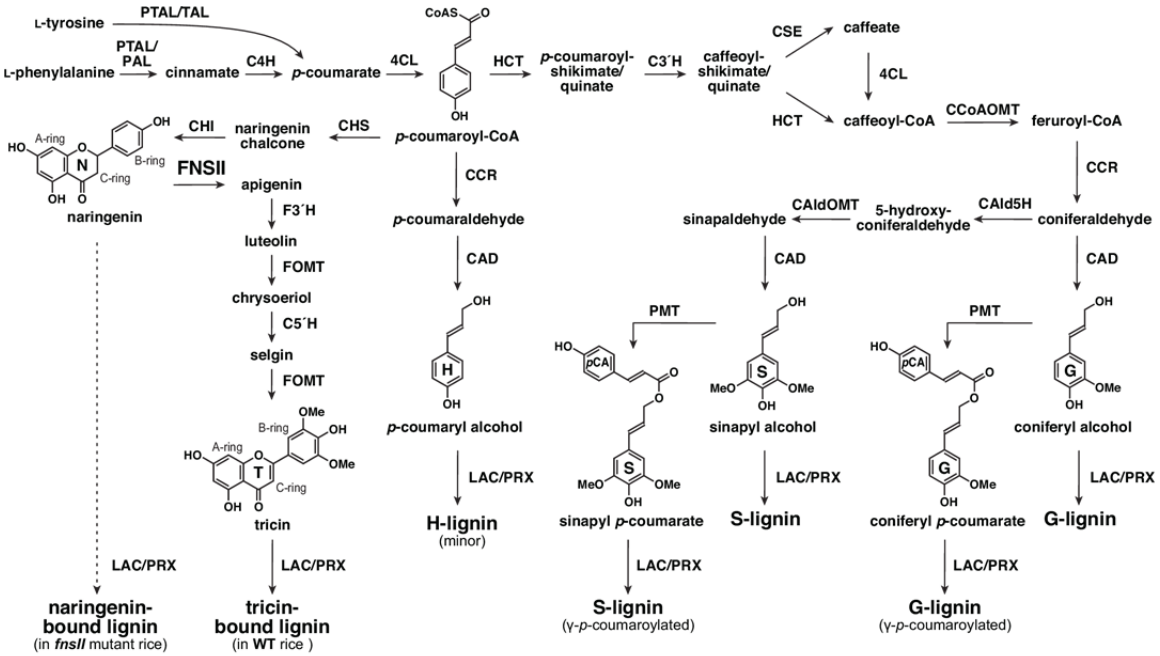

(DESIGNED IN DOUBLE-COLUMN SIZE)

Fig. 1. Proposed lignin biosynthetic pathway in grasses.

PTAL, phenylalanine and tyrosine ammonia lyase; TAL, tyrosine ammonia lyase; PAL, phenylalanine ammonia lyase; C4H, cinnamate 4-hydroxylase; 4CL, 4-coumarate CoA ligase; HCT, p-hydroxycinnamoyl-coenzyme A: quinate/shikimate *p*-hydroxycinnamoyltransferase; C3 ′ H, *p*-coumaroyl ester 3-hydroxylase; CSE, caffeoyl shikimate esterase; CCR, cinnamoyl-CoA reductase; CCoAOMT, caffeoyl-CoA O-methyltransferase; CAld5H, coniferaldehyde 5-hydroxylase; CAldOMT, 5-hydroxyconiferaldehyde O-methyltransferase; CAD, cinnamyl alcohol dehydrogenase; PMT, p-coumaroyl-CoA:monolignol transferase; CHS, chalcone synthase; CHI, chalcone isomerase; FNSII, flavone synthase II; F3 ′ H, flavonoid 3 ′ -hydroxylase; FOMT, flavonoid O-methyltransferase; C5′H, crysoeriol 5′-hydroxylase; LAC, laccase; PRX, peroxidase.

polysaccharides (cellulose and hemicelluloses), lignin confers increased mechanical strength, imperviousness, and resistance to pathogens (Boerjan et al., 2003; Bonawitz and Chapple, 2010; Umezawa, 2010). Lignin biosynthesis and bioengineering have long been a major research focus particularly because of its economic importance associated with agro-industrial utilizations of biomass. Lignin has traditionally been viewed as an impediment to chemical pulping, forage digestion by livestock, and cellulosic bioethanol production, but is increasingly viewed as a potent source for producing aromatic commodities from biomass. Accordingly, the phenylpropanoid pathway responsible for synthesizing monolignols that build up lignin polymers has been one of the major targets in cell wall bioengineering studies (Ragauskas et al., 2014; Beckham et al., 2016; Rinaldi et al., 2016).

The biosynthesis of monolignols from *p*-coumaroyl CoA involves aromatic hydroxylations and *O*-methylations as well as successive side-chain reductions to

generate the three canonical monolignols differing in their degree of aromatic methoxylation (Fig. 1) (Boerjan et al., 2003; Bonawitz and Chapple, 2010; Umezawa, 2010). In angiosperms, i.e., both in dicots and monocots, lignins are majorly composed of guaiacyl (G) and syringyl (S) units derived from combinational radical couplings, initiated by laccases and/or peroxidases, of two monolignols, coniferyl and sinapyl alcohols, respectively, with a lower amount of *p*-hydroxyphenyl (H) units from *p*-coumaryl alcohol (Boerjan et al., 2003; Bonawitz and Chapple, 2010; Umezawa, 2010). While sharing this typical lignin trait with dicots, lignins in the major monocot family Poaceae (grasses including cereals) are partially acylated at the γ-position with *p*-coumarate. It has been established that such lignin acylations arise from lignification with γ-*p*-coumaroylated monolignols generated by a grass specific acyltransferase, *p*-coumaroyl-CoA:monolignol transferase, PMT (Fig. 1) (Petrik et al., 2014). Furthermore, it was recently demonstrated that various commelinid monocots, including Poaceae species, also incorporate a small amount of γ-feruloylated monolignols for lignification (Karlen et al., 2016).

Flavonoids have been known to couple with monolignols, forming extractable flavonolignans, flavonolignols, and their *O*-glycosides. For example, silymarin extracted from milk thistle seeds contains flavonolignans derived from coupling of taxifolin and coniferyl alcohol (Kim et al., 2003; Wang et al., 2010). Hydnocarpin and 5′-methoxyhydnocarpin, coupling products of luteolin with coniferyl or sinapyl alcohol, were identified in *Hydnocarpus wightiana* (Parthasarathy et al., 1979), *Onopordon corymbosum* (Cardona et al., 1990) and *Hymeneae palustris* (Pettit et al., 2003). Other naturally occurring flavonolignans and flavonolignols include pseudotsuganol, hydnowightin, neohydnocarpin, palstatin, sinaiticin, and silandrin (Foo and Karchesy, 1989; Sharma et al., 1979; Pettit et al., 2003; Nyiredy et al., 2008). In monocots, the widespread nature and the high structural diversity of tricin-type flavonolignans and their related derivatives are well documented (Yang et al., 2013; Zhou and Ibrahim, 2010; Lan et al., 2016a; Li et al., 2016). More strikingly, after resolving the unknown signals in the NMR spectra of polymeric lignins isolated from wheat cell walls, tricin was recently discovered as an integrated component of lignins (Del Río et al., 2012). Subsequently, extensive surveys have revealed that tricin-bound lignins abundantly exist particularly in

the monocot family Poaceae, which comprises grasses including cereals. They have been also found in some commelinid monocot families outside Poaceae, such as Arecaceae (palms) and Bromeliaceae (pineapples and relatives), the non-commelinid family Orchidaceae (the orchids), particularly in the genus *Vanilla*, and also in certain dicots (Lan et al., 2015; Lan et al., 2016a; Lan et al., 2016b; Wen et al., 2013; Del Río et al., 2015; Rencoret et al., 2013; Koshiba et al., 2017).

Tricin, as an authentic lignin monomer in grasses, incorporates into the lignin polymers via combinational radical couplings, as in the way lignification takes place solely with monolignols in dicots and gymnosperms. Lacking the abilities to either undergo radical dehydrodimerization or to start the polymer chain elongations from the phloroglucinol A ring, tricin always occurs at one terminus of a lignin polymer chain, and was proposed to function as a nucleation site for lignification (Lan et al., 2015). The discovery of the tricin-bound lignins, illustrating the plasticity of lignification and its strong inter-connection with flavonoid biosynthesis, sheds a new light on the studies of lignin biosynthesis and bioengineering. Currently, however, it remains largely unknown how tricin-bound lignins are biosynthesized and function in grass cell walls. Given that many of the grass biomass crops, e.g., sorghum, sugarcane, switchgrass, and bamboo, produce substantial amounts of tricin-bound lignins (Lan et al., 2016b), it is also intriguing to investigate how tricin-bound lignins are affecting the utilization properties of cell walls.

We previously reported that a flavone synthase II (OsFNSII) is essential for the biosynthesis of extractable tricin metabolites, i.e. tricin *O*-glycosides and *O*-flavonolignans, in rice seedlings (Lam et al., 2014). OsFNSII, which catalyzes the direct conversion of flavanones to flavones, is a cytochrome P450 enzyme (CYP93G1) belonging to the grass-specific 93G subfamily. In the present study, we address the involvement of OsFNSII in lignification and examine cell wall properties upon tricin deficiency. A T-DNA insertional rice *fnsII* mutant was subjected to a series of analyses for assessment of growth phenotypes, gene expressions as well as lignin structure. A series of chemical analyses demonstrated that the mutant produced cell walls with reduced lignin levels and decreased syringyl/guaiacyl lignin unit composition. NMR characterizations revealed the complete depletion of tricin along with the incorporation of

naringenin, a flavanone substrate of OsFNSII, as a new component in cell wall lignin. Importantly, such lignin alterations resulted in enhanced cell wall digestibility without negative impact on growth and development. Together, our work establishes the essential role of OsFNSII in tricin lignification in cell wall and suggests that grass biomass utilization may be enhanced by manipulation of flavone biosynthesis pathway.

RESULTS

Expression of Flavonoid and Monolignol Biosynthetic Genes in Wild-type Rice Plants

At the onset of this study, we performed *in silico* gene expression analysis of flavonoid and monolignol biosynthetic genes in wild-type rice (*O. sativa* L. ssp. *japonica* cv. Nipponbare) (Sato et al., 2012). As with other putative/known tricin biosynthetic genes such as *OsCHS1* (Shih et al., 2008; Hong et al., 2012), *OsCHI* (Shih et al., 2008), and *OsC5′H* (CYP75B4; Lam et al., 2015), *OsFNSII* (CYP93G1; Lam et al., 2014) was most prominently expressed in culm at reproductive and ripening stages, where cell wall lignification is typically occurring; we confirmed concurrent expressions of putative/known monolignol biosynthetic genes including *OsCAD2* (Koshiba et al., 2013b, Zhang et al., 2006), *OsCAldOMT1* (Koshiba et al., 2013a), and *OsPMT* (Petrik et al., 2014) as well as the common phenylpropanoid genes including *OsPAL1/2* (Cass et al., 2015) and *Os4CL3* (Gui et al., 2011) (Supplemental Fig. S1). In addition, *OsFNSII*, along with its downstream *OsC5′H* (Fig. 1), was expressed in leaf at vegetative stage and also in lemma and palea at the later stage of flower development, and several monolignol biosynthetic genes displayed similar spatial and temporal expression patterns (Supplemental Fig. S1). These data support our contention that *OsFNSII* is involved not only in the biosynthesis of soluble tricin metabolites, e.g., tricin *O*-glycosides and *O*-flavonolignans (Lam et al., 2014), but also of tricin monomer for lignification in the major rice vegetative tissues, as further demonstrated below.

Phenotype of *OsFNSII*-knockout Mutant Rice

To further examine the involvement of OsFNSII in cell wall lignification, we reinvestigated a loss-of-function mutant rice (*O. sativa* L. ssp. *japonica* cv. Kitaake) which we characterized previously (Lam et al., 2014); this mutant has a T-DNA insertion in the second exon of the *OsFNSII* locus (Fig. 2A). Gene expression analysis on a homozygous mutant line (*fnsII*) using a quantitative real-time PCR (qRT-PCR) approach suggested that overall, with the exception of a slightly depressed *OsC5′H* expression, there are no significant changes in the major flavonoid and monolignol biosynthetic gene

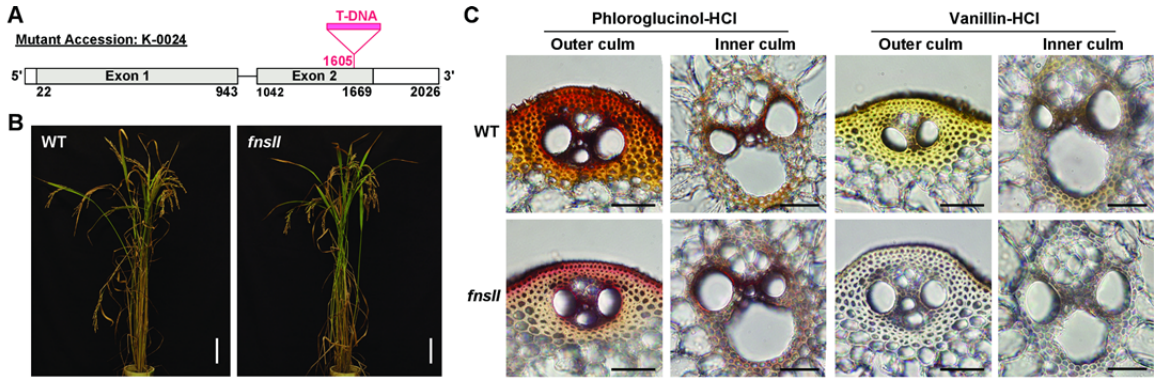

(DESIGNED IN DOUBLE-COLUMN SIZE)

Fig. 2. Gene structure, phenotype, and vasculature of *FNSII*-knockout mutant rice (*fnsII*) compared with a wild-type (WT) rice.
(A) Gene structure of *OsFNSII* (*CYP93G1*) in the T-DNA insertional mutant *fnsII* used in this study.
(B) Morphological phenotype of WT and *fnsII* mutant at harvest stage (45 days after heading). Scale bars denote 10 cm.
(C) Histochemical analysis of culm cell walls in WT and *fnsII* mutant at heading stage. Transverse cross sections of culms were stained by phloroglucinol-HCl and vanillin-HCl reagents for lignin and flavonoids, respectively. Scale bars denote 40 μm.

expressions compared to wild-type plants (Supplemental Fig. S2). The mutant plants grew to maturity without displaying significant morphological changes compared with the wild-type controls (Fig. 2B). Although a slight reduction in plant height was observed, *fnsII* plants overall displayed a similar growth performance comparable to wild-type plants in terms of their culm length, tillering, fertility, and biomass production, at least under the growth conditions used (Table I).

Histochemical Analysis of *OsFNSII*-knockout Mutant Rice Cell Walls

Transverse sections from developing culms of *fnsII* mutant and wild-type plants were subject to histochemical analyses using lignin and flavonoid staining reagents (Fig. 2C). As is the case with wild-type plants, *fnsII* mutants developed morphologically normal vascular tissues with thick secondary walls in the cortical sclerenchyma fibers and vascular bundles. The *fnsII* cell walls exhibited positive colorations with phloroglucinol-HCl (Wiesner reagent) that is known to react with cinnamaldehyde end-groups in the monolignol-derived lignin polymers. The staining of *fnsII* mutant cell walls, however, was apparently less intense than that of wild-type cell walls, indicating a decreased lignin content and/or a considerable alteration in lignin structure. In parallel, the sections were treated with vanillin-HCl, a well-known staining reagent for general flavonoid compounds (Gardner, 1975). The wild-type sections displayed a yellowish positive staining in the cortical sclerenchyma fibers and vascular bundle cell walls, suggesting a

substantial amount of flavonoid, presumably tricin, bound to the cell walls. In contrast, no obvious flavonoid staining was observed for the *fnsII* mutant cell walls, suggesting a considerable depletion of flavonoids in the cell walls (Fig. 2C). These histochemical data collectively suggest that *OsFNSII* disruption does not lead to defects in vascular morphology but potential reduction and/or alteration of flavonoid-bound lignins in cell walls.

Chemical Analysis of *OsFNSII*-knockout Mutant Rice Cell Walls

To investigate the cell wall chemotype of the *fnsII* mutant, we first performed a series of chemical analyses on extractive-free cell wall residues (CWRs) prepared from senesced culm, sheath, and leaf tissues; no significant differences were found in the yield of CWR per dry plant tissue between wild-type and *fnsII* mutant plants (Table I). Lignin content determined by thioglycolic acid assay was remarkably reduced, by 34-58%, in *fnsII* mutant cell walls compared to wild-type cell walls (Fig. 3A). This is in line with our earlier observation in the histochemical analysis (Fig. 2C). We also employed thioacidolysis to quantify lignin monomers released from monolignol-derived β–*O*–4 lignin substructures (Lapierre et al., 1986; Yamamura et al., 2012; Yue et al., 2012). The mutant cell walls released significantly less, by 17-33%, lignin monomers than wild-type cell walls upon thioacidolysis degradation (Fig. 3B), further confirming that *OsFNSII* disruption reduces the generation of lignins from monolignols. However, when the thioacidolysis monomer yield is expressed relative to lignin content, an opposite trend was observed in most of the samples (Supplemental Fig. S3). The total thioacidolysis-released H+G+S monomers and G monomers per thioglycolic lignin were significantly higher in all the tissues tested. Also, significant increases in S-type monomers in culm and leaf, and H-type monomers in leaf tissues were observed. Intriguingly, the *fnsII* mutant cell walls appeared to show a trend of decreased S/G monomer ratio in all the tissues tested (Fig. 3C and 3D). Taken together, our lignin analysis suggested that *OsFNSII* disruption somehow affects the content and composition of lignins derived from typical monolignols.

Cell wall-bound *p*-coumarates (*p*CAs) and ferulates (FAs) were quantified as the corresponding free acids released under mild alkaline hydrolysis of CWRs. The *fnsII*

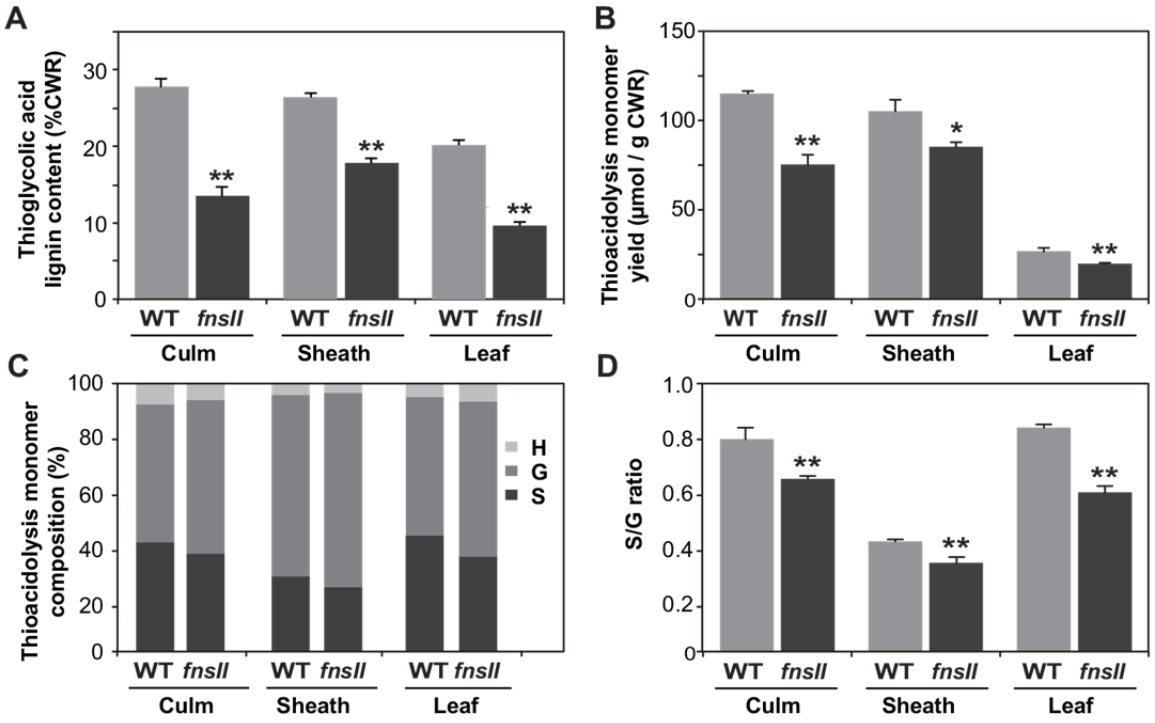

(DESIGNED IN SINGLE-AND-A-HALF-COLUMN SIZE)

Fig. 3. Chemical lignin analysis of cell walls from wild-type (WT) and *FNSII*-knockout mutant (*fnsII*) rice plants.

(A) Lignin content determined by thioglycolic acid assay.

(B), **(C)** and **(D)** Lignin composition analysis by thioacidolysis. Total monomer yield per cell wall residue, CWR **(B)** and relative abundances **(C** and **D)** of H, G, and S-type trithioethylpropane monomers released from H, G, and S-type lignins.

Values are means ± standard deviation (SD) from individually analyzed plants (n = 3), and asterisks indicate significant differences between WT and fnsII mutant plants (Student' s t-test, *: $p < 0.05$; **: $p < 0.01$).

mutant cell walls displayed significantly reduced *p*CA levels (25-48% less compared to wild-type controls) particularly in culm and sheath tissues (Fig. 4A), whereas FA levels were not significantly affected in all the vegetative tissues investigated (Fig. 4B). Given

that a majority of *p*CA is bound to lignins whereas FA mainly to hemicelluloses (arabinoxylans) in typical grass cell walls (Ralph, 2010), it is plausible that the reduced *p*CA levels in culm and sheath were associated with the reduced levels of lignins derived

261 from monolignols (Fig. 3). This was further supported by comparing the *p*CA content per
262 thioglycolic lignin between wild-type and the *fnsII* mutant plants (Supplemental Fig. S4):
263 there was no substantial difference on the content of *p*CA per lignin in the culm and

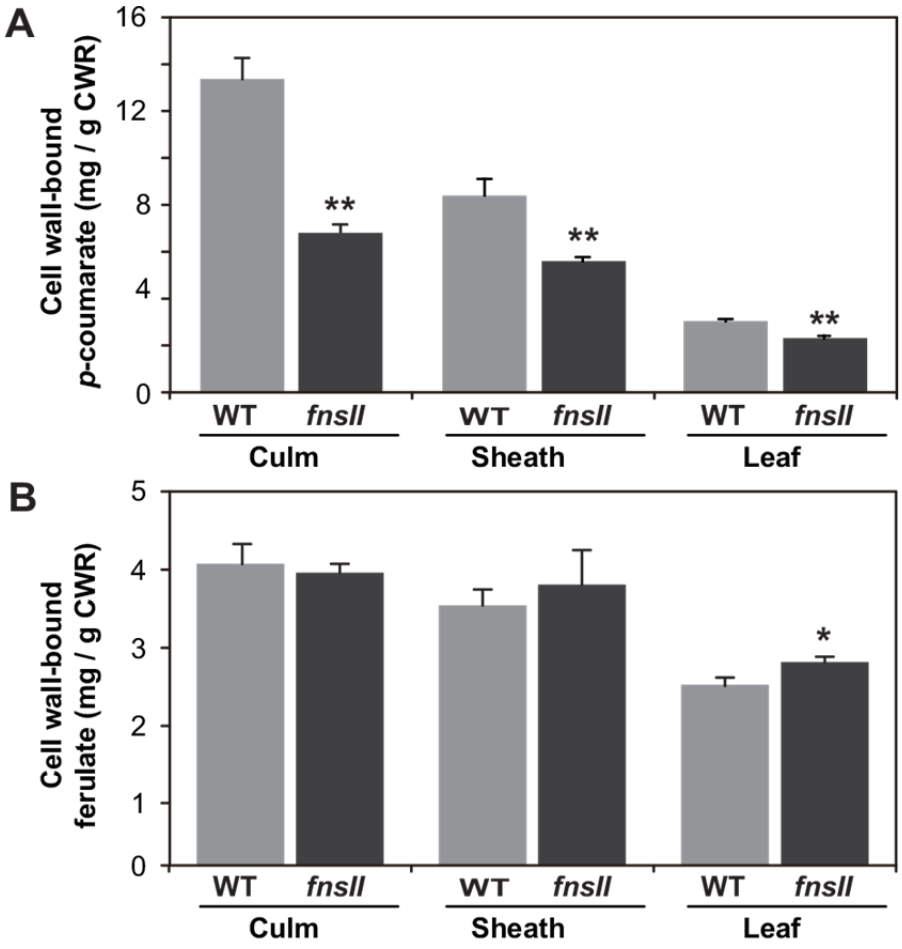

(DESIGNED IN SINGLE-COLUMN SIZE)

Fig. 4. Cell wall-bound p-coumarates **(A)** and ferulates **(B)** released from wild-type (WT) and *FNSII*-knockout mutant (*fnsII*) cell walls via mild alkaline hydrolysis. Values are means ± standard deviation (SD) from individually analyzed plants (n = 3), and asterisks indicate significant differences between WT and fnsII mutant plants (Student' s t-test, *: $p < 0.05$; **: $p < 0.01$). CWR, cell wall residue.

sheath tissues. We also analyzed cell wall sugar composition via a combination of trifluoroacetic acid and sulfuric acid-catalyzed cell wall hydrolysis reactions (see the experimental section). Overall, wild-type and *fnsII* mutant cell walls displayed similar

sugar profiles, suggesting that *OsFNSII* disruption does not affect the composition of cell wall polysaccharides; as is typical in grass cell walls, crystalline cellulose and arabinoxylans comprise a major part of cell wall polysaccharides in both wild-type and *fnsII* mutant tissues (Supplemental Fig. S5).

2D NMR Analysis of *OsFNSII*-knockout Mutant Rice Cell Walls

To further investigate the impact of *OsFNSII*-knockout mutation on cell wall structure, we performed 2D NMR analysis on the cell walls isolated from *fnsII* and wild-type culm tissues. We first analyzed whole cell wall materials by simple swelling of CWRs in dimethyl sulfoxide (DMSO)-d_6/pyridine-d_5 after fine ball-milling. This approach provides a global picture of the chemical composition and structure of cell wall lignins as well as polysaccharides (Mansfield et al., 2012; Kim and Ralph, 2010). For a more in-depth analysis, we analyzed lignin-enriched cell walls prepared from CWRs following enzymatic removal of polysaccharides (Tobimatsu et al., 2013; Zhao et al., 2013).

The aromatic sub-regions of the short range ^{1}H–^{13}C correlation (HSQC) NMR spectra displayed typical lignin aromatic signals from G and S units (**G** and **S**), as well as those from H units (**H**) albeit at low levels (Fig. 5 and Supplemental Fig. S6A). Volume integrations of these contour signals estimated 46-58% and 42-54% of S and G lignins, respectively (Fig. 5E). In line with our observation in thioacidolysis (Fig. 3D), S lignin signals were clearly depleted over G lignin signals in the *fnsII* mutant cell wall spectra. Besides the typical aromatic signals from the monolignol-derived lignins, the HSQC spectra of wild-type cell walls displayed the characteristic set of aromatic signals from lignin-bound tricin units (**T**); the chemical shifts of all the C–H correlations from the flavone aromatic system ($\mathbf{T_3}$, $\mathbf{T_{8/6}}$, and $\mathbf{T_{2'/6'}}$) are in total agreement with literature data (Del Río et al., 2012; Lan et al., 2015; Koshiba et al., 2017). In contrast, all these tricin signals were strikingly depleted to undetectable levels (<1 %) in the spectra of *fnsII* mutant cell walls (Fig. 5B and 5E). This clearly suggests that disruption of *OsFNSII* expression results in a strongly reduced incorporation of tricin into the lignin polymer.

In addition, a new set of aromatic signals appeared at δ_C/δ_H 95.0-96.5/6.2 in the *fnsII* mutant spectra. Based on the location of FNSII in the tricin biosynthetic pathway, we hypothesized that the new flavonoid-bound lignins could have been derived from

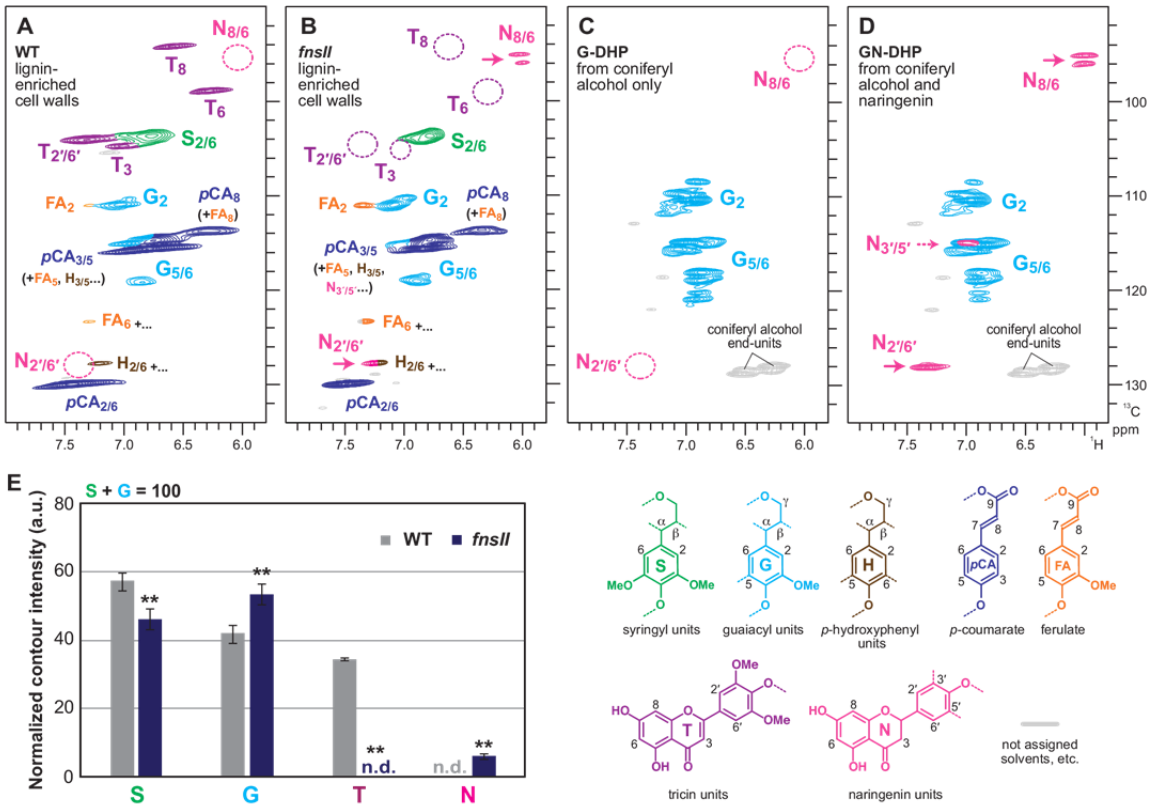

(DESIGNED IN DOUBLE-COLUMN SIZE)

Fig. 5. Aromatic sub-regions of short range ^{1}H–^{13}C correlation (HSQC) NMR spectra of cell wall lignins from culm tissues of wild-type (WT) and *FNSII*-knockout mutant (*fnsII*) rice plants, and *in vitro* synthetic lignin polymers (DHPs).

(A) and **(B)** Lignin-enriched cell walls of WT and fnsII mutant plants, prepared by enzymatic removal of wall polysaccharides with crude cellulases. Contour coloration matches that of the lignin substructure units shown.

(C) and **(D)** DHPs prepared from coniferyl alcohol only (G-DHP) and from coniferyl alcohol along with naringenin (GN-DHP). Contour coloration matches that of the lignin substructure units shown.

(E) Normalized contour intensity of the major lignin and flavonoid aromatic signals appearing in the spectra of lignin-enriched cell walls. The values are means ± standard deviation (SD) from individually analyzed plants (n = 3), and expressed as a percentage of the total of **S** and **G** lignin units. Asterisks indicate significant differences between WT and *fnsII* mutant plants (Student' s t-test, **: $p < 0.01$). n.d., not detected.

incorporating naringenin intermediate into the lignin polymers (Fig. 1). To test this hypothesis, we prepared synthetic lignin polymers (GN-DHP) via *in vitro* peroxidase-catalyzed copolymerization of naringenin and coniferyl alcohol. A close comparison of the NMR spectra of the mutant cell walls and GN-DHP firmly established the incorporation of naringenin into the lignin polymers (Fig. 5B and 5D). The resolved and diagnostic signals appearing at δ_C/δ_H 95.0-96.5/6.2 were assigned to C_8–H_8 and C_6–H_6 correlations of the naringenin flavanone aromatic system (**$N_{8/6}$**). Although the signals from naringenin B-ring were most likely overlapping with G and H lignin aromatic signals [$C_{2'}$–$H_{6'}$ correlations (**$N_{2'/6'}$**) at δ_C/δ_H ~128/~7.4; $C_{3'}$–$H_{5'}$ correlations (**$N_{3'/5'}$**) at

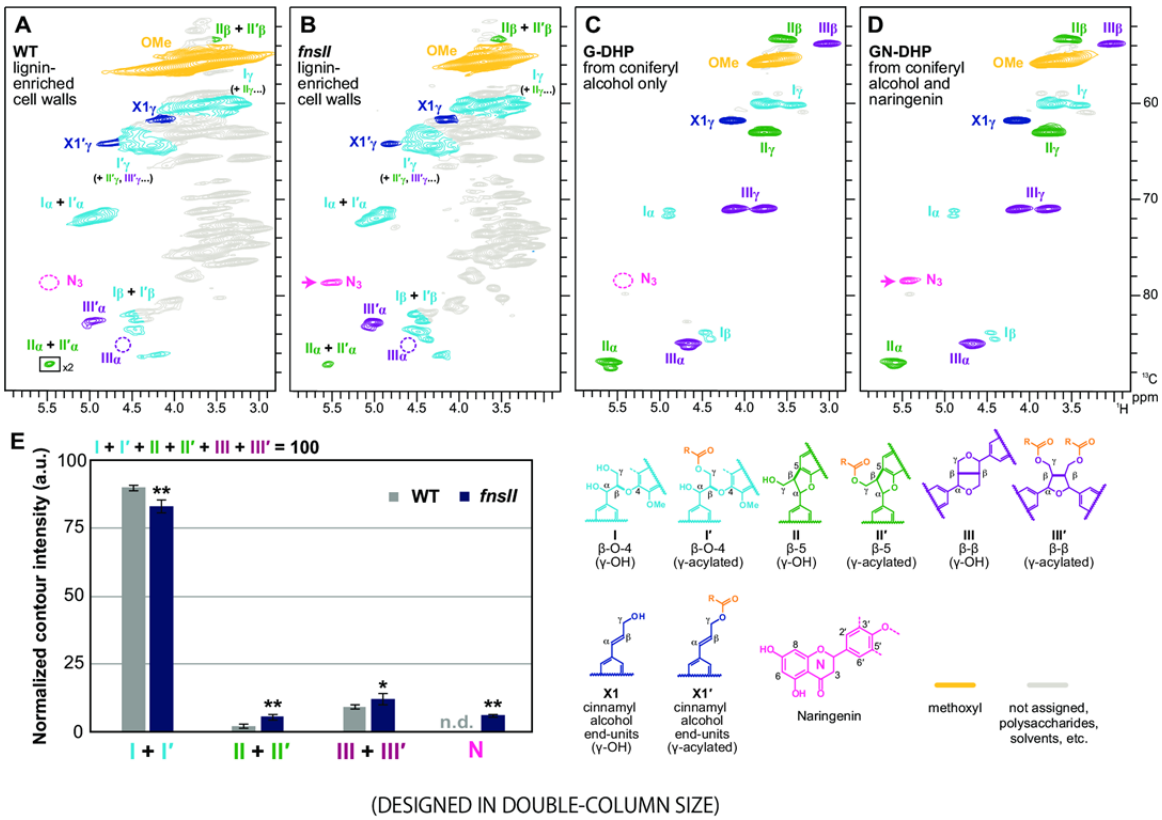

(DESIGNED IN DOUBLE-COLUMN SIZE)

Fig. 6. Aliphatic sub-regions of short range ^{1}H–^{13}C correlation (HSQC) NMR spectra of cell wall lignins from culm tissues of wild-type (WT) and *FNSII*-knockout 1mutant (*fnsII*) rice plants, and in vitro synthetic lignin polymers (DHPs).

(A) and **(B)** Lignin-enriched cell walls of WT and fnsII mutant plants, prepared by enzymatic removal of wall polysaccharides with crude cellulases. Boxes labeled x2 indicate regions that are vertically scaled 2-fold. Contour coloration matches that of the lignin substructure units shown.

(C) and **(D)** DHPs prepared from coniferyl alcohol only (G-DHP) and from coniferyl alcohol along with naringenin (GN-DHP). Contour coloration matches that of the lignin substructure units shown.

(E) Normalized contour intensity of the major lignin side-chain and naringenin signals appearing in the spectra of lignin-enriched cell walls. The values are means ± standard deviation (SD) from individually analyzed plants (n = 3), and expressed as a percentage of the total of **I**, **I′**, **II**, **II′**, **III**, and **III′** side-chain structures. Asterisks indicate significant differences between WT and fnsII mutant plants (Student' s t-test, *: $p < 0.05$; **: $p < 0.01$). n.d., not detected.

δ_C/δ_H ~115/~7.0], characteristic methylene signals from naringenin C-ring (**N_3**) were also well resolved and clearly seen at δ_C/δ_H 78.5/5.5 in the aliphatic sub-regions of the mutant and naringenin-incorporated GN-DHP spectra (Fig. 6 and Supplemental Fig. S6B).

The aliphatic sub-regions of the HSQC spectra also provide information of the major inter-monomeric linkages in the lignin polymers (Fig. 6 and Supplemental Fig. S6B). Typical lignin linkage signals from β–*O*–4 (**I**), β–5 (**II**), and β–β (**III**) units as well as those from the corresponding γ-acylated units (**I′**, **II′**, and **III′**) were visible in both wild-type and *fnsII* mutant cell wall spectra. Volume integrations of the relatively well-resolved C_α–H_α contours appearing in the lignin-enriched cell wall spectra allowed us to

estimate the distributions of these lignin inter-monomeric linkages (Fig. 6E). Our data suggested that the mutant lignins were significantly depleted in β-aryl ethers (**I**+**I´**) and augmented in phenylcoumarans (**II**+**II´**) and β–β (**III**+**III´**) units compared with wild-type lignins. As further discussed below, such shifts in the lignin linkage pattern might be a consequence of the reduction and partial replacement of tricin units by naringenin units. We also analyzed the profiles of cell wall polysaccharides based on the sugar anomeric correlations appearing in the whole cell wall spectra (Kim and Ralph, 2014; Brennan et al., 2012). Overall, distributions of the sugar correlations were similar between the wild-type and mutant spectra (Supplemental Fig. S6C), which is totally in line with the chemical data (Supplemental Fig. S5).

Digestibility of *OsFNSII*-knockout Mutant Rice Cell Walls

Lastly, to determine the effect of truncation of the tricin biosynthetic pathway on cell wall digestibility, we evaluated enzymatic saccharification efficiency of the rice cell walls. Pulverized and de-starched culm CWRs were digested, without any pretreatment, using a cocktail of commercially available cellulolytic enzymes (Hattori et al., 2012). Typical enzymatic hydrolysis profiles were obtained for both wild-type and mutant cell walls; saccharification was rapid during the first 6 h of hydrolysis and continued incubation released comparatively small amounts of additional glucose. As illustrated in Fig. 7, it was clearly observed that the mutant cell walls yielded more glucose than the wild-type controls at all the incubation times examined. The enhancement of saccharification efficiency was 25-30% when expressed as glucose yield per cell walls and 30-40% when expressed as glucose yield per total glucan.

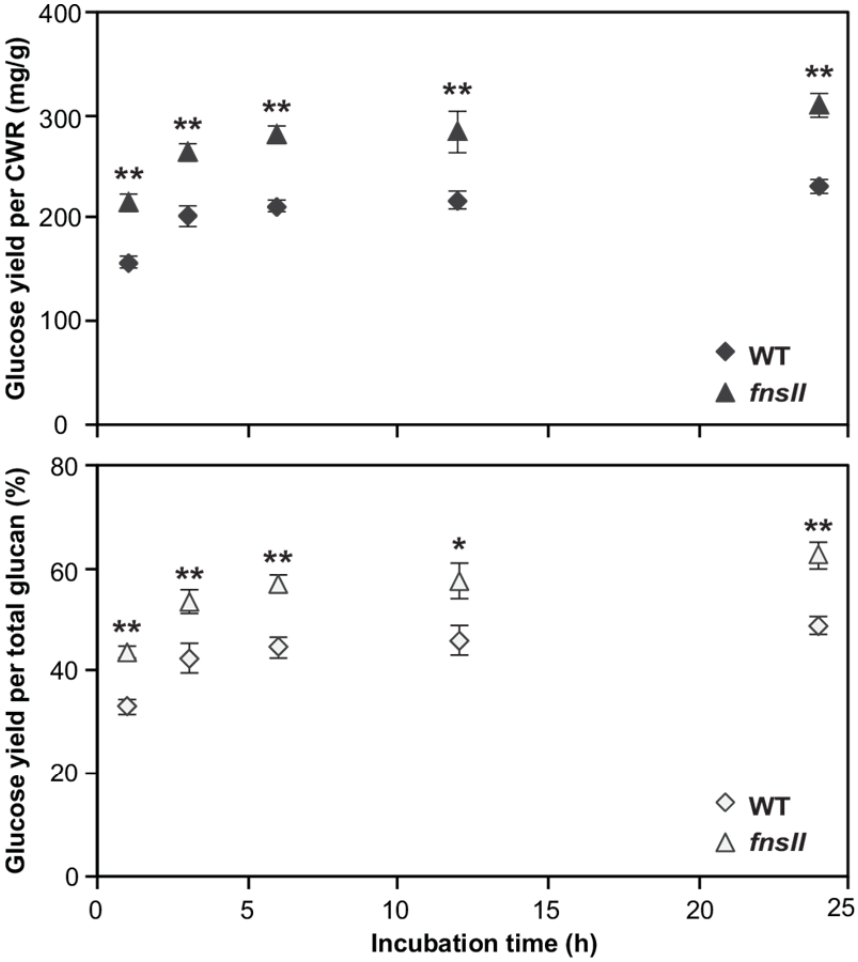

(DESIGNED IN SINGLE-COLUMN SIZE)

Fig. 7. Enzymatic saccharification of cell walls from culm tissues of wild-type (WT) and *FNSII*-knockout mutant (*fnsII*) rice plants. The saccharification efficiency is expressed as glucose yield per cell wall residue, CWR (upper), or as glucose yield per total glucan (bottom). Values are means ± standard deviation (SD) from individually analyzed plants (n = 3), and asterisks indicate significant differences between WT and fnsII mutant plants (Student' s t-test, *: $p < 0.05$; **: $p < 0.01$).

DISCUSSION

FNSII Mutant Rice Produces Cell Wall Lignins Devoid of Tricin

The tricin biosynthetic pathway in rice was completely elucidated recently with identification of a series of previously uncharacterized flavone enzymes (Kim et al., 2006; Lam et al., 2014 and 2015). Among them, OsFNSII (CYP93G1) represents a branch-point enzyme for the entry to tricin biosynthesis in rice (Lam et al., 2014). Grass FNSIIs classified in the CYP93G subfamily were likely to have evolved independently from dicot FNSIIs which belong to the 93B subfamily (Supplemental Fig. S7). Recombinant OsFNSII converts naringenin and eriodictyol into apigenin and luteolin, respectively. In addition, Arabidopsis over-expressing *OsFNSII* produces apigenin, luteolin and chrysoeriol *O*-glycosides, which are normally not produced in the tissues examined. Furthermore, the accumulation of extractable flavones, including tricin *O*-glycosides and *O*-flavonolignans, was compromised in the *fnsII* mutant. Hence, OsFNSII is indispensable for the production of extractable tricin metabolites in rice (Lam et al., 2014).

The present study provides compelling evidence that OsFNSII is also responsible for generating tricin monomer for cell wall lignification in rice. Our NMR analysis clearly demonstrated that the *fnsII* mutant produces cell wall lignins devoid of tricin residues. The tricin aromatic signals appearing in the HSQC spectra of the mutant cell walls are below detection limits (<1 %), while those signals account for about 34% relative to the total of G and S lignin signals in the wild-type cell walls (Fig. 5E). It should be noted here that, as recently reported (Lan et al., 2016b), such HSQC NMR-based estimates of tricin concentrations are most likely excessive; tricin is mostly in lignins as the polymers' terminal units and typical HSQC experiments over-quantify such more mobile terminal units compared with rigid internal units (Mansfield et al., 2012; Tobimatsu et al., 2013; Okamura et al., 2016). In fact, a recent study reported that tricin concentrations in grass lignins determined by a more reliable chemical method are typically 1-3% (Lan et al., 2016b). Given that all the tricin signals are below the detection limit in our HSQC NMR analysis for the *fnsII* mutant, it is conceivable that the actual concentration of lignin-bound tricin in this mutant is practically zero.

Interestingly, *FNSII*-mutation also impacted lignification of typical monolignols. Thioglycolic acid lignin assay estimated 34-58% lignin reductions in *fnsII* mutant cell walls compared to wild-type controls (Fig. 3A). In addition, we observed 18-35%

reductions in the total yields of monolignol monomers released upon thioacidolysis (Fig. 3B), suggesting that the apparent lignin reduction in the *fnsII* mutant was not only caused by the loss of tricin units, but also by the depletion in the lignin units derived from the canonical monolignols. This is also corroborated by the lower intensity of phloroglucinol-HCl lignin staining in vascular tissues (Fig. 2C) as well as the reductions in lignin-bound *p*CA levels (Fig. 4A). On the other hand, when the yield of thioacidolysis-released monolignol monomers was expressed relative to the thioglycolic lignin content, an increase was observed in the *fnsII* mutant (Supplemental Fig. S3), implying that the mutant lignin is less condensed. Apparently, this is contradictory to what was observed in our NMR analysis; the *fnsII* mutant contained less non-condensed β-aryl ethers and more phenylcoumaran and β-β units than the wild-type control (Fig. 6E). It could be partly due to the fact that, unlike NMR which provides structural information on the entire lignin, thioacidolysis analyzes only a fraction of the polymer containing cleavable β-aryl ethers; it is also reported that the acylation of lignin in grasses impedes the efficient cleavage of β-aryl ethers and thus the lignin monomer yield determined for grass samples under typical thioacidolysis conditions could be substantially underestimated (Grabber et al., 1996; Yue et al., 2012).

In addition to the reduced lignin levels, we also observed significantly decreased S/G lignin unit ratios in all the mutant tissues as determined by both thioacidolysis (Fig. 3D) and NMR (Fig. 5E). It has been reported that disruptions in the monolignol biosynthetic pathway redirect the metabolic flux in the phenylpropanoid pathway and occasionally affect accumulations of flavonoids (Besseau et al., 2007; Li et al., 2010; Fornalé et al., 2010; Abdlrazzak et al., 2006; Fornalé et al., 2015; Vanholme et al., 2012). It is therefore conceivable that a blockage in a flavonoid pathway may in turn affect the generation of monolignols and their lignin polymers. Very recently, it was reported that a maize mutant defective in CHS (Figure 1) produces tricin-depleted cell walls with a substantially increased total lignin content (Eloy et al., 2016), which is apparently in contrast to our *FNSII* rice mutant with lignins depleted in both tricin and monolignol-derived units. As CHS is the entry enzyme for the flavonoid pathway branching off from the general phenylpropanoid pathway (Figure 1), downregulation of *CHS* can redirect the carbon flux from the biosynthesis of flavonoids to canonical monolignols, which consequently results

406 in plants with increased lignin levels. Such scenario, however, may not prevail in our rice
407 *fnsII* mutant because FNSII functions in the downstream of the flavonoid pathways
408 (Figure 1). In fact, as further discussed below, *fnsII* mutant rice abnormally accumulates
409 narigenin-incorporated lignins as well as other narigenin-derived flavone and flavanone
410 metabolites as we previously reported (Lam et al., 2014). These data suggest that the
411 carbon flux redirected from the biosynthesis of tricin is at least partially compensated
412 within the flavonoid pathway. Although further studies are required, the reduction of
413 lignin content in the rice *fnsII* mutant may suggests a feedback system that controls the
414 relative carbon flux between flavonoid and monolignol biosynthetic pathways. It should
415 be also noted here that, unlike the case of *CHS*-defective maize (Eloy et al., 2016), *CHS*-
416 suppressions in some dicot species resulted in no alterations or, like in our *FNSII* rice
417 mutant, reductions in lignin levels (Li et al., 2010; Zuk et al., 2016). Therefore, cross-
418 interactions between the flavonoid and monolignol pathway metabolisms may also be
419 much dependent on different metabolic plasticity in different plant species.
420
421 **_FNSII_ Mutant Rice Incorporates Naringenin as A Novel Lignin Component**
422 An intriguing discovery in this study was that loss of tricin for lignification in the *fnsII*
423 mutant was partially compensated by incorporating naringenin, a flavanone substrate of
424 FNSII, as a new component of lignin polymer units (Fig. 1). In line with this, we
425 previously reported over-accumulation of soluble naringenin metabolites in the *fnsII*
426 mutant seedlings (Lam et al., 2014). The successful generation of synthetic lignin
427 polymer (GN-DHP) from naringenin and coniferyl alcohol *in vitro* indicates that
428 naringenin is compatible in lignin polymerization; naringenin has a capability to be
429 radicalized by peroxidases, cross-coupled with monolignols, and integrally incorporated
430 into the lignin polymers. Our NMR analysis also demonstrated that the lignin-linked
431 naringenin residues still contain the intact phloroglucinol A-rings (Fig. 5 and 6). This
432 suggests that reactions of *p*-hydroxyphenyl B-ring far exceed A-ring reactions during
433 lignin polymerization with naringenin. Previous studies examining chemical and
434 enzymatic oxidations of tricin (Lan et al., 2015) and analogous flavonoids (Elumalai et al,
435 2012; Grabber et al., 2012; Itoh et al., 2007) also have reported predominant reactions of
436 cinnamoyl B-rings over phloroglucinol-type A-rings. Furthermore, these NMR data can

be also interpreted that the newly incorporated naringenin units are linked majorly as the terminal units of the lignin polymer chains, as is proposed for the canonical tricin units (Lan et al., 2015).

Tricin bearing the 3′,5′-dimethoxyl-*p*-hydroxyphenyl B-ring incorporates into lignin exclusively via 4′–*O*–β-type coupling, which ultimately creates β-aryl ether units in the lignin polymer chains (Fig. 8A) (Lan et al., 2015). On the other hand, naringenin with non-substituted *p*-hydroxyphenyl B-ring logically can couple with monolignols not only via 4′–*O*–β-type coupling for β-aryl ether units (Fig. 8B) but also via 3′–β-type coupling, yielding additional phenylcoumaran units at the lignin terminus (Fig. 8C). Therefore, our observation that *fnsII* mutant lignins had notably increased phenylcoumaran units (about 3-fold increase, based on HSQC signal integrations, Fig. 6E) could be partially explained by the replacement of tricin lignin monomer by naringenin.

As envisioned by the histochemical analysis with the vanillin-HCl reagent (Fig. 2C), the incorporation of naringenin into *fnsII* mutant lignins was unlikely to reach the level of tricin incorporation in wild-type lignins. In our HSQC analysis, whereas tricin signals account for ~35 % relative to the total of G and S lignin signals in the wild-type cell wall spectra, naringenin signals have reached only about 6 % in the *fnsII* mutant spectra (Fig. 5E). Our previous metabolite study also suggested a relatively lower level of soluble naringenin metabolites in *fnsII* mutant seedlings compared to soluble tricin metabolites in wild-type seedlings (Lam et al., 2014). Meanwhile, *OsFNSII* disruption may also increase carbon flow to the production of flavone *C*-glycosides through CYP93G2 which utilize naringenin as a substrate (Lam et al., 2014; Du et al., 2010a).

Extensive studies on the biosynthesis and bioengineering of lignin have revealed the plasticity of lignification *in planta*. Manipulation of the canonical monolignol pathway had led to compositional alterations in the polymer due to incorporation of non-traditional lignin monomers, e.g., caffeyl alcohol in a *CCoAOMT*-deficient plant (Wagner et al., 2011), 5-hydroxyconiferyl alcohol in *CAldOMT*-deficient plants (Jouanin et al., 2000; Ralph et al., 2001; Vanholme et al., 2010; Weng et al., 2010; Koshiba et al., 2013a), ferulic acid in *CCR*-deficient plants (Ralph et al., 2008; Wagner et al., 2013), and *p*-hydroxycinnamaldehydes in *CAD*-deficient plants (Kim et al., 2000; Marita et al.,

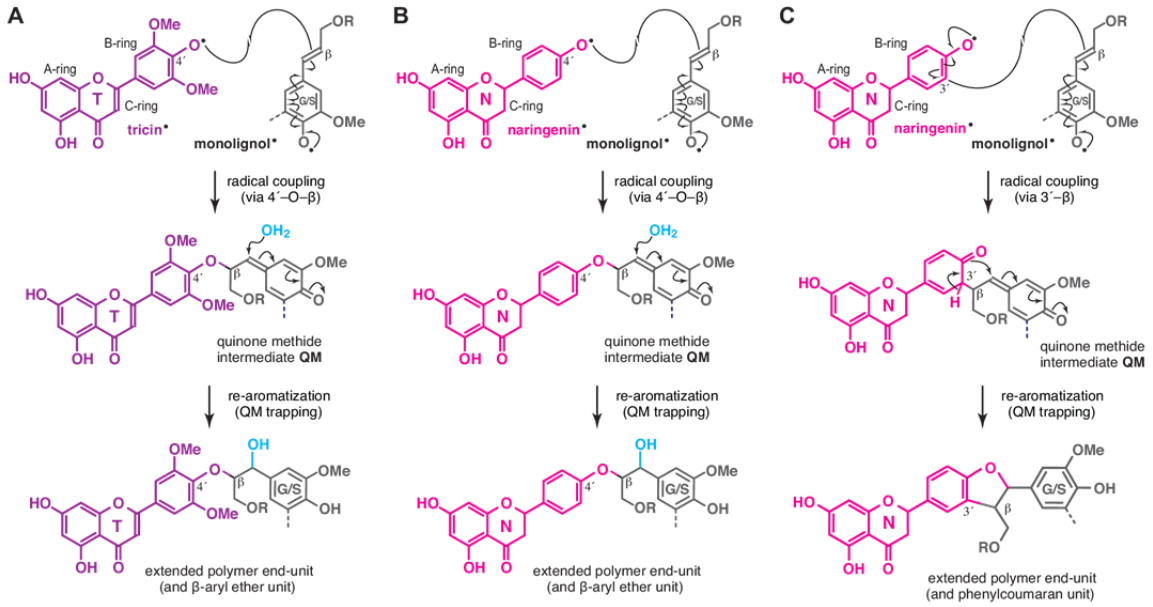

(DESIGNED IN DOUBLE-COLUMN SIZE)

Fig. 8. Generation of flavonoid-bound lignin units upon lignification.

(A) The 4′–O–β pathway for β-aryl units via cross-coupling of tricin and monolignols upon lignification in wild-type rice cell walls.

(B) and **(C)** The 4′–O–β and 3′–β pathways for β-aryl ether and phenylcoumaran units via cross-coupling of naringenin and monolignols upon lignification in fnsII mutant rice cell walls.

2003; Sibout et al., 2005; Koshiba et al., 2013b; Bouvier d'Yvoire et al., 2013; Zhao et al., 2013; Anderson et al., 2015). Such malleability of lignification is also exemplified by the fact that numerous angiosperm plants produce seed coat-specific lignins derived from caffeyl and 5-hydroxyconiferyl alcohols (Chen et al., 2012; 2013; Tobimatsu et al., 2013). Our discovery that *FNSII*-deficiency in rice results in incorporation of naringenin into lignin further illustrates the substantial flexibility in the construction of lignin polymers *in planta*.

FNSII Mutant Rice is Viable and Produces Biomass with an Improved Digestibility

As the quantity and quality of lignin affect many aspects of lignocellulosic biomass utilization, regulation of lignin biosynthesis has been a primary target for cell wall bioengineering (Ragauskas et al., 2014; Beckham et al., 2016; Rinaldi et al., 2016). During biofuels production, lignin is a major recalcitrant barrier to the enzymatic saccharification of cell wall polysaccharides. Reduction of lignin content and/or alteration of lignin composition can improve the efficiency of enzymatic cell wall hydrolysis and downstream microbial fermentations (Chen and Dixon, 2007). However,

such lignin modifications often result in developmental abnormalities, such as collapsed xylem, stunted growth, and infertility (Bonawitz and Chapple 2013). Importantly, despite with a considerably reduced lignin content and altered flavonoid-bound lignins, the *fnsII* mutant develops apparently intact vascular tissues (Fig. 2C) and displays overall normal plant growth, biomass production, and fertility, all comparable with the wild-type controls (Table I). Likewise, the recently reported tricin-depleted maize *CHS*-mutant displayed no growth defects (Eloy et al., 2016). Although a more comprehensive analysis on plant growth performance under various stress conditions should be examined in the future, it is implicated that the absence of integrated tricin in lignins is unlikely a major detrimental factor for growth and development at least in rice and maize. At the same time, the *fnsII* mutant exhibits a remarkably enhanced cell wall digestibility (Fig. 7). Considering that tricin actually takes up small portions of rice cell walls (Lan et al. 2016b), the improved enzymatic saccharification efficiency of the rice *fnsII* mutant could be attributed mainly to the reduced lignin levels. On the contrary, the tricin-depleted maize *CHS*-mutant showed a substantially reduced saccharification efficiency, which was in turn attributed to the increased lignin levels (Eloy et al., 2016). Taken together, lignin content, rather than an absence or modification of lignin-bound tricin units, is likely a major factor affecting the saccharification efficiency observed for the tricin-truncated mutant plants.

Overall, we envision that genetic manipulations of tricin biosynthesis could be an alternative strategy to engineer grass cell walls for efficient biomass conversion processes without severely compromising plant fitness. Given that the CYP93G members (FNSIIs) are highly conserved in Poaceae (Lam et al., 2014; Supplemental Fig. S7), there is a strong potential to extend the application to bioenergy grass crops such as sorghum, sugarcane, switchgrass, and bamboo. Meanwhile, further generation of transgenic rice plants with altered flavonoid compositions in lignin will facilitate the elucidation of the physiology functions and phylogeny of tricin-bound lignins in grasses.

MATERIALS AND METHODS

Plant Materials

Rice T-DNA insertion mutant of CYP93G1 (accession: K-00244; cv Kitaake) was obtained originally from the Crop Biotech Institute of Kyung Hee University. Rice seeds were surface sterilized, germinated and grown in a phytotoron under a 12 h photoperiod and ~30 ºC day / ~24 ºC night temperature regime. The wild-type and *fnsII* homozygous mutant plants were isolated by a genomic PCR approach as described previously (Lam et al., 2014), and primers used for genotyping are listed in Supplemental Table S1. Mature plants (45 days after the heading) were used for phenotypic characterization, harvested, and dried in a temperature controlled room (27 ºC, for 30 days) prior to cell wall characterization.

Gene Expression Analysis

Total RNA was extracted individually from lignifying culms of rice plants at the heading stage as described previously (Koshiba et al., 2013b) and reverse-transcribed into cDNA using random hexamer (Invitrogen, Carlsbad, CA, USA) as a primer. Gene expression assayed used an Applied Biosystems 7300 Real-time PCR System (Applied Biosystems, Forester City, CA, USA) and primer sets listed in Supplemental Table S1. An ubiquitin gene (*OsUBQ5*; AK061988) was used as an internal control. Microarray-based gene expression data for *in silico* gene expression analysis (Supplemental Fig. S1) were retrieved from the Rice Expression Profile Database (RiceXPro) (Sato et al., 2012).

Histochemical Analysis

Fresh hand-cut specimens (~8 mm) were excised from culms at the heading stage, fixed in formaldehyde/propionic acid/ethanol at a ratio of 3.7:5:50 (v/v/v), treated with ethanol/acetic acid at a ratio of 6:1 (v/v) to remove extractives, and agarose-embedded. Sections were sliced at 100 μm-thickness using a DTK-2000 microslicer (Dosaka EM, Kyoto, Japan). For lignin staining using the phloroglucinol-HCl method, sections were incubated in 1 % (w/v) phloroglucinol in ethanol for 10 min and acidified in 17.5 N HCl for 10 min. For flavonoid staining using the vanillin-HCl method, sections were incubated in 1 % (w/v) vanillin in ethanol for 10 min followed by incubation in 17.5 N

HCl for 10 min. The sections treated were then observed under an Olympus BX51 microscope (Olympus Optical, Tokyo, Japan).

Cell Wall Preparations

Extractive-free cell wall residues (CWRs) for chemical analysis and NMR were prepared as previously described (Yamamura et al., 2012). Briefly, dried rice plant tissues were pulverized with a TissueLyser (Qiagen, Hilden, Germany), extracted sequentially with methanol, hexane, and distilled water, and then freeze-dried to give CWRs. For NMR analysis, CWRs (~300 mg) were further ball-milled using a planetary micro mill Pulverisette 7 (Fritsch Industrialist, Idar-Oberstein, Germany) with ZrO_2 vessels containing ZrO_2 ball bearings (600 rpm, 12 cycles of 10 min at 5 min intervals) (Mansfield et al., 2012; Tobimatsu et al., 2013). For whole cell wall NMR analysis, 60 mg of the ball-milled CWRs was directly swelled in 600 µl DMSO-d_6/pyridine-d_5 (4:1, v/v). In parallel, ~240 mg of the ball-milled CWRs was further digested with crude cellulases (Cellulysin, Calbiochem, La Jolla, CA, USA) according to the methods described previously (Tobimatsu et al., 2013). The obtained lignin-enriched CWRs (ca. 40-60 mg) were dissolved in 600 µl DMSO-d_6/pyridine-d_5 (4:1, v/v) and subjected for NMR analysis.

Chemical Analysis

Lignin content was estimated by thioglycolic acid method (Suzuki et al., 2009). Analytical thioacidolysis was performed according to the method described previously (Yamamura et al., 2012), and the released lignin monomers were derivatized with *N*,*O*-bis(trimethylsilyl)acetamide and quantified by gas chromatography/mass spectrometry (GC/MS) using 4,4′-ethylenebisphenol as an internal standard (Yue et al., 2012). Cell wall-bound *p*CA and FA were quantified using the methods described by Yamamura et al. (2011). The monosaccharide composition of the cell-wall polysaccharides, excluding crystalline cellulose, was determined by hydrolysing CWRs with trifluoroacetic acid and analyzing the released monosaccharides as alditol acetates by GC/MS with inositol acetate as an internal standard (Chen et al., 2012). Crystalline cellulose content of the residue was determined by washing it with the Updegraff reagent (Updegraff, 1969)

followed by a complete hydrolysis with 72% sulfuric acid (Hattori et al., 2012) and glucose quantified by Glucose CII test kit (Wako Pure Chemicals Industries, Osaka, Japan).

Generation of Synthetic Lignin Polymers

Dehydrogenation polymer (DHPs) from coniferyl alcohol and naringenin was generated by the so-called bulk polymerization method (Tobimatsu et al., 2008; 2011). Briefly, 100 ml of acetone/sodium phosphate buffer (0.1 M, pH 6.5) (1:9, v/v) containing 0.5 mmol of coniferyl alcohol (for G-DHP) or 0.425 mmol of coniferyl alcohol together with 0.075 mmol of naringenin (for GN-DHP), along with 100 ml of hydrogen peroxide solution (0.6 mmol) were separately added to 25 ml sodium phosphate buffer (pH 6.5) containing 5 mg horseradish peroxidase (HRP, Type IV, Sigma-Aldrich, St. Louis, MO, USA) over 1 h at room temperature. The solution was further stirred for 14 h and the precipitates formed were collected by centrifugation (13,640 g, 15 min), washed with distilled water (50 ml × 4), and lyophilized to afford G-DHP (~53 mg, 59 % weight yield) or GN-DHP (~37 mg, 38% weight yield) as colorless powders. The DHPs (~30 mg) were dissolved in 600 μl DMSO-d_6/pyridine-d_5 (4:1, v/v) for NMR analysis.

2D NMR analysis

NMR spectra were acquired on a Bruker Biospin Avance III 800US system (Bruker Biospin, Billerica, MA, USA) equipped with a cryogenically cooled 5-mm TCI gradient probe. Adiabatic heteronuclear single-quantum coherence (HSQC) NMR experiments were carried out using standard implementation ("hsqcgcep.3") with parameters described in the literature (Mansfield et al., 2012). Data processing and analysis used Bruker TopSpin 3.1 software (Bruker Biospin, Billerica, MA, USA), and the central DMSO solvent peaks (δ_C/δ_H: 39.5/2.49 ppm) were used as an internal reference. HSQC plots were obtained with typical matched Gaussian apodization in F2 and squared cosine-bell apodization and one level of linear prediction (32 coefficients) in F1. For volume integration, linear prediction was turned off and no correction factors were used. For integration of lignin and flavonoid aromatic signals (Fig. 5), C_2–H_2 correlations from guaiacyl units (**G**) and C_2–H_2/C_6–H_6 correlations from syringyl units (**S**), $C_{2'}$–$H_{2'}$/$C_{6'}$–$H_{6'}$

correlations from tricin (**T**), and C_8–H_8/C_6–H_6 correlations from naringenin (**N**) residues were used, and the **S**, **T**, and **N** integrals were logically halved. For integrations of lignin inter-monomeric linkages (Fig. 6), well-resolved C_α–H_α contours from **I**, **I′**, **II**, **II′**, **III**, and **III′** units, and C_3–H_3 contours from **N** were integrated, and **III**, **III′**, and **N** integrals were logically halved. The relative contour intensities listed in Fig. 5E and Fig. 6E are derived from three biological replicates and expressed on **G** + **S** = 100 and **I** + **I′** + **II** + **II′** + **III** + **III′** = 100 bases, respectively.

Determination of Enzymatic Saccharification Efficiency

Enzymatic saccharification efficiency was determined essentially by the method described in Hattori et al. (2012). Briefly, CWRs were destarched and subjected to enzymatic hydrolysis with a cellulolytic enzyme cocktail composed of Celluclast 1.5 L, Novozyme 188, and Ultraflo L (Novozymes, Bagsvaerd, Denmark) in a sodium citrate buffer (pH 4.8). Glucose concentration at each incubation time point was determined by Glucose CII test kit (Wako Pure Chemicals Industries, Osaka, Japan). Cellulose content for calculation of cellulose-to-glucose conversion was independently determined by hydrolysis of destarched CWRs with sulfuric acid (Hattori er al., 2012).

Phylogenetic Analysis

The unrooted phylogenetic tree was constructed by neighbor-joining method using MEGA6 (Tamura et al., 2013) with default parameters. Bootstrapping with 1,000 replications was performed.

Accession Numbers

Sequence data from this article can be found in the EMBL/GenBank data libraries under accession number(s) AK100972 (*OsFNSII*, LOC_Os04g01140). Accession numbers for the sequences used in the phylogenetic analysis were shown in the tree or in the legend of Supplemental Fig. S7.

ACKNOWLEDGMENTS

637 We thank Mr. Naoyuki Matsumoto, Ms. Keiko Tsuchida and Ms. Megumi Ozaki for
638 assisting in the analysis of rice cell walls, Dr. Hironori Kaji and Ms. Ayaka Maenofor
639 their assistance in NMR analysis, and also Dr. Arata Yoshinaga and Dr. Keiji Takabe for
640 their assistance and helpful suggestions for histochemical analysis. A part of this study
641 was conducted using the facilities in the DASH/FBAS at the Research Institute for
642 Sustainable Humanosphere, Kyoto University, and the NMR spectrometer in the JURC at
643 the Institute for Chemical Research, Kyoto University.
644

645 **TABLES**

646

647 **Table I.** Growth phenotypes, biomass yield and fertility rate of wide-type (WT) and *fnsII*
648 mutant plants.
649

Trait	WT	*fnsII*
Plant Height (cm) [a]	115.0±4.7	105.1±6.0*
Culm length (cm) [b]	86.3±5.3	79.7±7.5
Ear length (cm)	16.0±2.5	15.3±1.1
Tiller number	10.4±1.7	12.2±3.4
Ear number	14.6±2.0	14.8±2.6
Dry mass of culm (g)	4.8±1.4	3.7±0.7
Dry mass of sheath (g)	3.2±0.5	3.6±1.3
Dry mass of leaf (g)	3.0±0.4	3.8±1.1
CWR yield of culm (%) [c]	63.2±6.5	62.8±2.5
CWR yield of sheath (%) [c]	84.7±0.7	80.2±6.4
CWR yield of leaf (%) [c]	73.6±0.99	70.1±4.66
Number of panicles	15.0±2.2	15.4±2.7
Average mass per panicle (g)	1.1±0.2	1.2±0.2
Fertility rate (%)	85.3±3.9	83.6±2.7

650 Values are means ± SD (n = 5), and asterisks (*) indicate significant difference from WT
651 (Student's t-test, $p < 0.05$). [a]Length from cotyledonary node to the tip of the top leaf.
652 [b]Length from cotyledonary node to panicle base. [c]CWR, cell wall residue.

FIGURE LEGENDS

Fig. 1. Proposed lignin biosynthetic pathway in grasses.

PTAL, phenylalanine and tyrosine ammonia lyase; TAL, tyrosine ammonia lyase; PAL, phenylalanine ammonia lyase; C4H, cinnamate 4-hydroxylase; 4CL, 4-coumarate CoA ligase; HCT, *p*-hydroxycinnamoyl-coenzyme A: quinate/shikimate *p*-hydroxycinnamoyltransferase; C3′H, *p*-coumaroyl ester 3-hydroxylase; CSE, caffeoyl shikimate esterase; CCR, cinnamoyl-CoA reductase; CCoAOMT, caffeoyl-CoA *O*-methyltransferase; CAld5H, coniferaldehyde 5-hydroxylase; CAldOMT, 5-hydroxyconiferaldehyde *O*-methyltransferase; CAD, cinnamyl alcohol dehydrogenase; PMT, *p*-coumaroyl-CoA:monolignol transferase; CHS, chalcone synthase; CHI, chalcone isomerase; FNSII, flavone synthase II; F3′H, flavonoid 3′-hydroxylase; FOMT, flavonoid *O*-methyltransferase; C5′H, crysoeriol 5′-hydroxylase; LAC, laccase; PRX, peroxidase.

Fig. 2. Gene structure, phenotype, and vasculature of *FNSII*-knockout mutant rice (*fnsII*) compared with a wild-type (WT) rice.

(A) Gene structure of *OsFNSII* (*CYP93G1*) in the T-DNA insertional mutant *fnsII* used in this study.

(B) Morphological phenotype of WT and *fnsII* mutant at harvest stage (45 days after heading). Scale bars denote 10 cm.

(C) Histochemical analysis of culm cell walls in WT and *fnsII* mutant at heading stage. Transverse cross sections of culms were stained by phloroglucinol-HCl and vanillin-HCl reagents for lignin and flavonoids, respectively. Scale bars denote 40 μm.

Fig. 3. Chemical lignin analysis of cell walls from wild-type (WT) and *FNSII*-knockout mutant (*fnsII*) rice plants.

(A) Lignin content determined by thioglycolic acid assay.

(B), **(C)** and **(D)** Lignin composition analysis by thioacidolysis. Total monomer yield per cell wall residue, CWR **(B)** and relative abundances **(C** and **D)** of H, G, and S-type trithioethylpropane monomers released from H, G, and S-type lignins.

Values are means ± standard deviation (SD) from individually analyzed plants ($n = 3$), and asterisks indicate significant differences between WT and *fnsII* mutant plants (Student's *t*-test, *: $p < 0.05$; **: $p < 0.01$).

Fig. 4. Cell wall-bound *p*-coumarates **(A)** and ferulates **(B)** released from wild-type (WT) and *FNSII*-knockout mutant (*fnsII*) cell walls via mild alkaline hydrolysis. Values are means ± standard deviation (SD) from individually analyzed plants ($n = 3$), and asterisks indicate significant differences between WT and *fnsII* mutant plants (Student's *t*-test, *: $p < 0.05$; **: $p < 0.01$). CWR, cell wall residue.

Fig. 5. Aromatic sub-regions of short range $^{1}H–^{13}C$ correlation (HSQC) NMR spectra of cell wall lignins from culm tissues of wild-type (WT) and *FNSII*-knockout mutant (*fnsII*) rice plants, and *in vitro* synthetic lignin polymers (DHPs).

(A) and **(B)** Lignin-enriched cell walls of WT and *fnsII* mutant plants, prepared by enzymatic removal of wall polysaccharides with crude cellulases. Contour coloration matches that of the lignin substructure units shown.
(C) and **(D)** DHPs prepared from coniferyl alcohol only (G-DHP) and from coniferyl alcohol along with naringenin (GN-DHP). Contour coloration matches that of the lignin substructure units shown.
(E) Normalized contour intensity of the major lignin and flavonoid aromatic signals appearing in the spectra of lignin-enriched cell walls. The values are means ± standard deviation (SD) from individually analyzed plants ($n = 3$), and expressed as a percentage of the total of **S** and **G** lignin units. Asterisks indicate significant differences between WT and *fnsII* mutant plants (Student's *t*-test, **: $p < 0.01$). n.d., not detected.

Fig. 6. Aliphatic sub-regions of short range $^{1}H–^{13}C$ correlation (HSQC) NMR spectra of cell wall lignins from culm tissues of wild-type (WT) and *FNSII*-knockout mutant (*fnsII*) rice plants, and *in vitro* synthetic lignin polymers (DHPs).
(A) and **(B)** Lignin-enriched cell walls of WT and *fnsII* mutant plants, prepared by enzymatic removal of wall polysaccharides with crude cellulases. Boxes labeled x2 indicate regions that are vertically scaled 2-fold. Contour coloration matches that of the lignin substructure units shown.
(C) and **(D)** DHPs prepared from coniferyl alcohol only (G-DHP) and from coniferyl alcohol along with naringenin (GN-DHP). Contour coloration matches that of the lignin substructure units shown.

(E) Normalized contour intensity of the major lignin side-chain and naringenin signals appearing in the spectra of lignin-enriched cell walls. The values are means ± standard deviation (SD) from individually analyzed plants (n = 3), and expressed as a percentage of the total of **I**, **I′**, **II**, **II′**, **III**, and **III′** side-chain structures. Asterisks indicate significant differences between WT and *fnsII* mutant plants (Student's *t*-test, *: $p < 0.05$; **: $p < 0.01$). n.d., not detected.

Fig. 7. Enzymatic saccharification of cell walls from culm tissues of wild-type (WT) and *FNSII*-knockout mutant (*fnsII*) rice plants. The saccharification efficiency is expressed as glucose yield per cell wall residue, CWR (upper), or as glucose yield per total glucan (bottom). Values are means ± standard deviation (SD) from individually analyzed plants (n = 3), and asterisks indicate significant differences between WT and *fnsII* mutant plants (Student's *t*-test, *: $p < 0.05$; **: $p < 0.01$).

Fig. 8. Generation of flavonoid-bound lignin units upon lignification.
(A) The 4′–O–β pathway for β-aryl units via cross-coupling of tricin and monolignols upon lignification in wild-type rice cell walls.
(B) and **(C)** The 4′–O–β and 3′–β pathways for β-aryl ether and phenylcoumaran units via cross-coupling of naringenin and monolignols upon lignification in *fnsII* mutant rice cell walls.

Supplemental Data

The following materials are available in the online version of this article.

Supplemental Fig. S1. Gene expression data of flavonoid and monolignol biosynthetic genes in wild-type rice plants.

Supplemental Fig. S2. Relative expression levels of flavonoid and monolignol biosynthetic genes in *fnsII* mutant culms.

Supplemental Fig. S3. Thioacidolysis yield per thioglycolic lignin content in wild-type and *fnsII* mutant rice tissues.

Supplemental Fig. S4. Cell wall-bound *p*-coumarates content per thioglycolic lignin content in wild-type and *fnsII* mutant rice tissues.

Supplemental Fig. S5. Sugar composition in wild-type and *fnsII* mutant rice tissues.

754 **Supplemental Fig. S6**. HSQC NMR spectra of the whole culm cell walls from wild-
755 type and *fnsII* mutant rice.
756 **Supplemental Fig. S7**. Phylogenetic tree of CYP93 proteins.
757 **Supplemental Table S1.** Primers used in this study.
758
759
760
761

Parsed Citations

Abdulrazzak N, Pollet B, Ehlting J, Larsen K, Asnaghi C, Ronseau S, Proux C, Erhardt M, Seltzer V, Renou J-P, Ullmann P, Pauly M, Lapierre C, Werck-Reichhart D (2006) A coumaroyl-ester-3-hydroxylase insertion mutant reveals the existence of nonredundant meta-hydroxylation pathways and essential roles for phenolic precursors in cell expansion and plant growth. Plant Physiol 140: 30-48

Pubmed: Author and Title
CrossRef: Author and Title
Google Scholar: Author Only Title Only Author and Title

Agati G, Azzarello E, Pollastri S, Tattini M (2012). Flavonoids as antioxidants in plants: location and functional significance. Plant Sci 196: 67-76

Pubmed: Author and Title
CrossRef: Author and Title
Google Scholar: Author Only Title Only Author and Title

Anderson NA, Tobimatsu Y, Ciesielski PN, Ximenes E, Ralph J, Donohoe BS, Ladisch M, Chapple C (2015) Manipulation of guaiacyl and syringyl monomer biosynthesis in an Arabidopsis cinnamyl alcohol dehydrogenase mutant results in atypical lignin biosynthesis and modified cell wall structure. Plant Cell 27: 2195-2209

Pubmed: Author and Title
CrossRef: Author and Title
Google Scholar: Author Only Title Only Author and Title

Barros J, Serrani-Yarce JC, Chen F, Baxter D, Venables BJ, Dixon RA (2016) Role of bifunctional ammonia-lyase in grass cell wall biosynthesis. Nat Plants 2: 16050

Pubmed: Author and Title
CrossRef: Author and Title
Google Scholar: Author Only Title Only Author and Title

Beckham GT, Johnson CW, Karp EM, Salvachúa D, Vardon DR (2016) Opportunities and challenges in biological lignin valorization. Curr Opin Biotechnol 42: 40-53

Pubmed: Author and Title
CrossRef: Author and Title
Google Scholar: Author Only Title Only Author and Title

Besseau S, Hoffmann L, Geoffroy P, Lapierre C, Pollet B, Legrand M (2007) Flavonoid accumulation in Arabidopsis repressed in lignin synthesis affects auxin transport and plant growth. Plant Cell 191: 148-162

Pubmed: Author and Title
CrossRef: Author and Title
Google Scholar: Author Only Title Only Author and Title

Boerjan W, Ralph J, Baucher M (2003) Lignin biosynthesis. Annu Rev Plant Biol 54: 519-546

Pubmed: Author and Title
CrossRef: Author and Title
Google Scholar: Author Only Title Only Author and Title

Bonawitz ND, Chapple C (2010) The genetics of lignin biosynthesis: connecting genotype to phenotype. Annu Rev Genet 44: 337-363

Pubmed: Author and Title
CrossRef: Author and Title
Google Scholar: Author Only Title Only Author and Title

Bonawitz ND, Chapple C (2013) Can genetic engineering of lignin deposition be accomplished without an unacceptable yield penalty? Curr Opin Biotechnol 24: 336-343

Pubmed: Author and Title
CrossRef: Author and Title
Google Scholar: Author Only Title Only Author and Title

Bouvier d'Yvoire M, Bouchabke-Coussa O, Voorend W, Antelme S, Cézard L, Legée F, Lebris P, Legay S, Whitehead C, McQueen-Mason SJ, Gomez LD, Jouanin L, Lapierre C, Sibout R (2013) Disrupting the cinnamyl alcohol dehydrogenase 1 gene (BdCAD1) leads to altered lignification and improved saccharification in Brachypodium distachyon. Plant J 73: 496-508

Pubmed: Author and Title
CrossRef: Author and Title
Google Scholar: Author Only Title Only Author and Title

Brennan M, McLean JP, Altaner C, Ralph J, Harris PJ (2012) Cellulose microbril angles and cell-wall polymers in different wood types of Pinus radiata. Cellulose 19: 1385-1404

Pubmed: Author and Title
CrossRef: Author and Title
Google Scholar: Author Only Title Only Author and Title

Cardona ML, Garcia B, Pedro JR, Sinisterra JF (1990) Flavonoids, flavonolignans and a phenylpropanoid from Onopordon corymbosum. Phytochemistry 29: 629-631

Pubmed: Author and Title
CrossRef: Author and Title
Google Scholar: Author Only Title Only Author and Title

Cass CL, Peraldi A, Dowd PF, Mottiar Y, Santoro N, Karlen SD, Bukhman YV, Foster CE, Thrower N, Bruno LC, Moskvin OV, Johnson ET, Willhoit ME, Phutane M, Ralph J, Mansfield SD, Nicholson P, Sedbrook JC (2015) Effects of PHENYLALANINE

AMMONIA LYASE (PAL) knockdown on cell wall composition, biomass digestibility, and biotic and abiotic stress responses in Brachypodium. J Exp Bot 66: 4317-4335
Pubmed: Author and Title
CrossRef: Author and Title
Google Scholar: Author Only Title Only Author and Title

Chen F, Dixon RA (2007) Lignin modification improves fermentable sugar yields for biofuel production. Nat Biotechnol 25: 759-761
Pubmed: Author and Title
CrossRef: Author and Title
Google Scholar: Author Only Title Only Author and Title

Chen F, Tobimatsu Y, Havkin-Frenkel D, Dixon RA, Ralph J (2012) A polymer of caffeyl alcohol in plant seeds. Proc Natl Acad Sci 109: 1772-1777
Pubmed: Author and Title
CrossRef: Author and Title
Google Scholar: Author Only Title Only Author and Title

Chen F, Tobimatsu Y, Jackson L, Nakashima J, Ralph J, Dixon RA (2013) Novel seed coat lignins in the Cactaceae: Structure, distribution and implications for the evolution of lignin diversity. Plant J 73: 201-211
Pubmed: Author and Title
CrossRef: Author and Title
Google Scholar: Author Only Title Only Author and Title

Del Rio JC, Lino AG, Colodette JL, Lima CF, Gutiérrez A, Martínez ÁT, Lu F, Ralph J, Rencoret J (2015) Differences in the chemical structure of the lignins from sugarcane bagasse and straw. Biomass Bioenerg 81:322-338
Pubmed: Author and Title
CrossRef: Author and Title
Google Scholar: Author Only Title Only Author and Title

Del Río JC, Rencoret J, Prinsen P, Martínez ÁT, Ralph J, Gutiérrez A (2012) Structural characterization of wheat straw lignin as revealed by analytical pyrolysis, 2D-NMR, and reductive cleavage methods. J Agric food chem 60: 5922-5935
Pubmed: Author and Title
CrossRef: Author and Title
Google Scholar: Author Only Title Only Author and Title

Dixon RA, Achnine L, Kota P, Liu C-J, Reddy MSS, Wang L (2002) The phenylpropanoid pathway and plant defence—a genomics perspective. Mol Plant Pathol 3: 371-390
Pubmed: Author and Title
CrossRef: Author and Title
Google Scholar: Author Only Title Only Author and Title

Dong X, Chen W, Wang W, Zhang H, Liu X, Luo J (2014) Comprehensive profiling and natural variation of flavonoids in rice. J Integr Plant Biol 56: 876-886
Pubmed: Author and Title
CrossRef: Author and Title
Google Scholar: Author Only Title Only Author and Title

Du Y, Chu H, Chu IK, Lo C (2010a) CYP93G2 is a flavanone 2-hydroxylase required for C-glycosyl-flavone biosynthesis in rice. Plant Physiol 154: 324-333
Pubmed: Author and Title
CrossRef: Author and Title
Google Scholar: Author Only Title Only Author and Title

Du Y, Chu H, Wang M, Chu IK, Lo C (2010b) Identification of flavone phytoalexins and a pathogen-inducible flavone synthase II gene (SbFNSII) in sorghum. J Exp Bot 61: 983-994
Pubmed: Author and Title
CrossRef: Author and Title
Google Scholar: Author Only Title Only Author and Title

Eloy N, Voorend W, Lan W, Saleme MdLS, Cesarino I, Vanholme R, Smith RA, Goeminne G, Pallidis A, Morreel K, Nicomedes J, Ralph J, Boerjan WA (2016) Silencing chalcone synthase impedes the incorporation of tricin in lignin and increases lignin content. Plant Physiol doi:01108.02016
Pubmed: Author and Title
CrossRef: Author and Title
Google Scholar: Author Only Title Only Author and Title

Elumalai S, Tobimatsu Y, Grabber JH, Pan X, Ralph, J (2012) Epigallocatechin gallate incorporation into lignin enhances the alkaline delignification and enzymatic saccharification of cell walls. Biotechnol Biofuels 5: 59
Pubmed: Author and Title
CrossRef: Author and Title
Google Scholar: Author Only Title Only Author and Title

Foo LY, Karchesy J (1989) Pseudotsuganol, a biphenyl-linked pinoresinol-dihydroquercetin from douglas-fir bark: isolation of the first true flavonolignan. J Chem Soc Chem Commun 217-219
Pubmed: Author and Title
CrossRef: Author and Title
Google Scholar: Author Only Title Only Author and Title

Fornalé S, Rencoret J, Garcia-Calvo L, Capellades M, Encina A, Santiago R, Rigau J, Gutiérrez A, del Río J-C, Caparros-Ruiz D (2015) Cell wall modifications triggered by the down-regulation of Coumarate 3-hydroxylase-1 in maize. Plant Sci 236: 272-282

Pubmed: Author and Title
CrossRef: Author and Title
Google Scholar: Author Only Title Only Author and Title

Fornalé S, Shi X, Chai C, Encina A, Irar S, Capellades M, Fuguet E, Torres J-L, Rovira P, Puigdomenech P, Rigau J, Erich Grotewold E, Gray J, Caparrós-Ruiz D (2010) ZmMYB31 directly represses maize lignin genes and redirects the phenylpropanoid metabolic flux. Plant J 64: 633-644
Pubmed: Author and Title
CrossRef: Author and Title
Google Scholar: Author Only Title Only Author and Title

Gardner RO (1975) Vanillin-hydrochloric acid as a histochemical test for tannins. Stain Technol 50: 315-317
Pubmed: Author and Title
CrossRef: Author and Title
Google Scholar: Author Only Title Only Author and Title

Goto T, Kondo T (1991) Structure and molecular stacking of anthocyanins—flower color variation. Angew Chem Int Ed 30: 17-33
Pubmed: Author and Title
CrossRef: Author and Title
Google Scholar: Author Only Title Only Author and Title

Grabber JH, Quideau S, Ralph J (1996) p-Coumaroylated syringyl units in maize lignin: Implications for ß-ether cleavage by thioacidolysis. Phytochem 43: 1189-1194
Pubmed: Author and Title
CrossRef: Author and Title
Google Scholar: Author Only Title Only Author and Title

Grabber JH, Ress D, Ralph J (2012) Identifying new lignin bioengineering targets: impact of epicatechin, quercetin glycoside, and gallate derivatives on the lignification and fermentation of maize cell walls. J Agric Food Chem 60: 5152-5160
Pubmed: Author and Title
CrossRef: Author and Title
Google Scholar: Author Only Title Only Author and Title

Gui J, Shen J, Li L (2011) Functional characterization of evolutionarily divergent 4-coumarate: coenzyme A ligases in rice. Plant Physiol 157: 574-586
Pubmed: Author and Title
CrossRef: Author and Title
Google Scholar: Author Only Title Only Author and Title

Hassan S, Mathesius U (2012) The role of flavonoids in root-rhizosphere signalling: opportunities and challenges for improving plant-microbe interactions. J Exp Bot 63: 3429-3444
Pubmed: Author and Title
CrossRef: Author and Title
Google Scholar: Author Only Title Only Author and Title

Hattori T, Murakami S, Mukai M, Yamada T, Hirochika H, Ike M, Tokuyasu K, Suzuki S, Sakamoto M, Umezawa T (2012) Rapid analysis of transgenic rice straw using near-infrared spectroscopy. Plant Biotechnol 29: 359-366
Pubmed: Author and Title
CrossRef: Author and Title
Google Scholar: Author Only Title Only Author and Title

Hong L, Qian Q, Tang D, Wang K, Li M, Cheng Z (2012) A mutation in the rice chalcone isomerase gene causes the golden hull and internode 1 phenotype. Planta 236: 141-151
Pubmed: Author and Title
CrossRef: Author and Title
Google Scholar: Author Only Title Only Author and Title

Itoh N, Katsube Y, Yamamoto K, Nakajima N, Yoshida K (2007) Laccase-catalyzed conversion of green tea catechins in the presence of gallic acid to epitheaflagallin and epitheaflagallin 3-O-gallate. Tetrahedron 63: 9488-9492
Pubmed: Author and Title
CrossRef: Author and Title
Google Scholar: Author Only Title Only Author and Title

Jouanin L, Goujon T, de Nadai V, Martin M-T, Mila I, Vallet C, Pollet B, Yoshinaga A, Chabbert B, Petit-Conil M, Lapierre C (2000) Lignification in transgenic poplars with extremely reduced caffeic acid O-methyltransferase activity. Plant Physiol 123: 1363-1374
Pubmed: Author and Title
CrossRef: Author and Title
Google Scholar: Author Only Title Only Author and Title

Karlen SD, Zhang C, Peck ML, Smith RA, Padmakshan D, Helmich KE, Free HCA, Lee S, Smith BG, Lu F, Sedbrook JC, Sibout R, Grabber JH, Runge TM, Mysore KS, Harris PJ, Bartley LE, Ralph J (2016) Monolignol ferulate conjugates are naturally incorporated into plant lignins. Sci Adv 2: e1600393
Pubmed: Author and Title
CrossRef: Author and Title
Google Scholar: Author Only Title Only Author and Title

Kim B-G, Lee Y, Hur H-G, Lim Y, Ahn J-H (2006) Flavonoid 3´-O-methyltransferase from rice: cDNA cloning, characterization and functional expression. Phytochemistry 67: 387-394
Pubmed: Author and Title
CrossRef: Author and Title
Google Scholar: Author Only Title Only Author and Title

Kim H, Ralph J (2010) Solution-state 2D NMR of ball-milled plant cell wall gels in DMSO-d6/pyridine-d5. Org Biomol Chem 8: 576-591
Pubmed: Author and Title
CrossRef: Author and Title
Google Scholar: Author Only Title Only Author and Title

Kim H, Ralph, J (2014). A gel-state 2D-NMR method for plant cell wall profiling and analysis: a model study with the amorphous cellulose and xylan from ball-milled cotton linters. RSC Adv 4: 7549-7560
Pubmed: Author and Title
CrossRef: Author and Title
Google Scholar: Author Only Title Only Author and Title

Kim H, Ralph J, Yahiaoui N, Pean M, Boudet A-M (2000) Cross-coupling of hydroxycinnamyl aldehydes into lignins. Org Lett 2: 2197-2200
Pubmed: Author and Title
CrossRef: Author and Title
Google Scholar: Author Only Title Only Author and Title

Kim N-C, Graf TN, Sparacino CM, Wani MC, Wall ME (2003) Complete isolation and characterization of silybins and isosilybins from milk thistle (Silybum marianum). Org Biomol Chem 1: 1684-1689
Pubmed: Author and Title
CrossRef: Author and Title
Google Scholar: Author Only Title Only Author and Title

Koes RE, Quattrocchio F, Mol JNM (1994) The flavonoid biosynthetic pathway in plants: function and evolution. Bioessays 16: 123-132
Pubmed: Author and Title
CrossRef: Author and Title
Google Scholar: Author Only Title Only Author and Title

Koshiba T, Hirose N, Mukai M, Yamamura M, Hattori T, Suzuki S, Sakamoto M, Umezawa T (2013a) Characterization of 5-hydroxyconiferaldehyde O-methyltransferase in Oryza sativa. Plant Biotechnol 30: 157-167
Pubmed: Author and Title
CrossRef: Author and Title
Google Scholar: Author Only Title Only Author and Title

Koshiba T, Murakami S, Hattori T, Mukai M, Takahashi A, Miyao A, Hirochika H, Suzuki S, Sakamoto M, Umezawa T (2013b) CAD2 deficiency causes both brown midrib and gold hull and internode phenotypes in Oryza sativa L. cv. Nipponbare. Plant Biotechnol 30: 365-373
Pubmed: Author and Title
CrossRef: Author and Title
Google Scholar: Author Only Title Only Author and Title

Koshiba T, Yamamoto N, Tobimatsu Y, Yamamura M, Suzuki S, Hattori T, Mukai M, Noda S, Shibata D, Sakamoto M, Umezawa T (2017) MYB-mediated upregulation of lignin biosynthesis in Oryza sativa towards biomass refinery. Plant Biotechnol, in press (DOI: 10.5511/plantbiotechnology.16.1201a)
Pubmed: Author and Title
CrossRef: Author and Title
Google Scholar: Author Only Title Only Author and Title

Lam PY, Liu H, Lo C (2015) Completion of tricin biosynthesis pathway in rice: Cytochrome P450 75B4 is a novel chrysoeriol 5'-hydroxylase. Plant Physiol 168: 1527-1536
Pubmed: Author and Title
CrossRef: Author and Title
Google Scholar: Author Only Title Only Author and Title

Lam PY, Zhu F-Y, Chan WL, Liu H, Lo C (2014) CYP93G1 is a flavone synthase II which channels flavanones to the biosynthesis of tricin O-linked conjugates in rice. Plant Physiol 165: 1315-1327
Pubmed: Author and Title
CrossRef: Author and Title
Google Scholar: Author Only Title Only Author and Title

Lan W, Lu F, Regner M, Zhu Y, Rencoret J, Ralph SA, Zakai UI, Morreel K, Boerjan W, Ralph J (2015) Tricin, a flavonoid monomer in monocot lignification. Plant Physiol 167: 1284-1295
Pubmed: Author and Title
CrossRef: Author and Title
Google Scholar: Author Only Title Only Author and Title

Lan W, Morreel K, Lu F, Rencoret J, del Río JC, Voorend W, Vermerris W, Boerjan WA, Ralph J (2016a) Maize tricin-oligolignol metabolites and their implications for monocot lignification. Plant Physiol 171: 810-820
Pubmed: Author and Title
CrossRef: Author and Title
Google Scholar: Author Only Title Only Author and Title

Lan W, Rencoret J, Lu F, Karlen SD, Smith BG, Harris PJ, del Río JC, Ralph J (2016b) Tricin-lignins: occurrence and quantitation of tricin in relation to phylogeny. Plant J, doi:10.1111/tpj.13315
Pubmed: Author and Title
CrossRef: Author and Title
Google Scholar: Author Only Title Only Author and Title

Lapierre C, Monties B, Roland C (1986) Preparative thioacidlysis of spruce lignin: isolation and identification of main monomeric products. Holzforschung 40: 47-50
Pubmed: Author and Title
CrossRef: Author and Title
Google Scholar: Author Only Title Only Author and Title

Li M, Pu Y, Yoo CG, Ragauskas AJ (2016) The occurrence of tricin and its derivatives in plants. Green Chem 18: 1439-1454
Pubmed: Author and Title
CrossRef: Author and Title
Google Scholar: Author Only Title Only Author and Title

Li X, Bonawitz ND, Weng J-K, Chapple C (2010) The growth reduction associated with repressed lignin biosynthesis in Arabidopsis thaliana is independent of flavonoids. Plant Cell 22: 1620-1632
Pubmed: Author and Title
CrossRef: Author and Title
Google Scholar: Author Only Title Only Author and Title

Mansfield SD, Kim H, Lu F, Ralph J (2012) Whole plant cell wall characterization using solution-state 2D NMR. Nat Protoc 7: 1579-1589
Pubmed: Author and Title
CrossRef: Author and Title
Google Scholar: Author Only Title Only Author and Title

Marita JM, Vermerris W, Ralph J, Hatfield RD (2003) Variations in the cell wall composition of maize brown midrib mutants. J Agric Food Chem 51: 1313-1321
Pubmed: Author and Title
CrossRef: Author and Title
Google Scholar: Author Only Title Only Author and Title

Nyiredy S, Samu Z, Szücs Z, Gulácsi K, Kurtán T, Antus S (2008) New insight into the biosynthesis of flavanolignans in the white-flowered variant of Silybum marianum. J Chromatogr Sci 46: 93-96
Pubmed: Author and Title
CrossRef: Author and Title
Google Scholar: Author Only Title Only Author and Title

Okamura H, Nishimura H, Nagata T, Kigawa T, Watanabe T, Katahira M (2016) Accurate and molecular-size-tolerant NMR quantitation of diverse components in solution. Sci Rep 6: 21742
Pubmed: Author and Title
CrossRef: Author and Title
Google Scholar: Author Only Title Only Author and Title

Parthasarathy MR, Ranganathan KR, Sharma D (1979) 13C NMR of flavonolignans from Hydnocarpus wightiana. Phytochemistry 18: 506-508
Pubmed: Author and Title
CrossRef: Author and Title
Google Scholar: Author Only Title Only Author and Title

Petrik DL, Karlen SD, Cass CL, Padmakshan D, Lu F, Liu S, Le Bris P, Antelme S, Santoro N, Wilkerson CG, Sibout R, Lapierre C, Ralph J (2014) p-Coumaroyl-CoA:monolignol transferase (PMT) acts specifically in the lignin biosynthetic pathway in Brachypodium distachyon. Plant J 77: 713-726
Pubmed: Author and Title
CrossRef: Author and Title
Google Scholar: Author Only Title Only Author and Title

Pettit GR, Meng Y, Stevenson CA, Doubek DL, Knight JC, Cichacz Z, Pettit RK, Chapuis J-C, Schmidt JM (2003) Isolation and Structure of Palstatin from the Amazon Tree Hymeneae palustris. J Nat Prod 66: 259-262
Pubmed: Author and Title
CrossRef: Author and Title
Google Scholar: Author Only Title Only Author and Title

Ragauskas AJ, Beckham GT, Biddy MJ, Chandra R, Chen F, Davis MF, Davison BH, Dixon RA, Gilna P, Keller M, Langan P, Naskar AK, Saddler JN, Tschaplinski TJ, Tuskan GA, Wyman CE (2014) Lignin valorization: improving lignin processing in the biorefinery. Science 344: 1246843
Pubmed: Author and Title
CrossRef: Author and Title
Google Scholar: Author Only Title Only Author and Title

Ralph J (2010) Hydroxycinnamates in lignification. Phytochem Rev 9: 65-83
Pubmed: Author and Title
CrossRef: Author and Title
Google Scholar: Author Only Title Only Author and Title

Ralph J, Kim H, Lu F, Grabber JH, Leplé JC, Berrio-Sierra J, Derikvand MM, Jouanin L, Boerjan W, Lapierre C (2008) Identification of the structure and origin of a thioacidolysis marker compound for ferulic acid incorporation into angiosperm lignins (and an indicator for cinnamoyl CoA reductase deficiency). Plant J 53: 368-379
Pubmed: Author and Title
CrossRef: Author and Title
Google Scholar: Author Only Title Only Author and Title

Ralph J, Lapierre C, Lu F, Marita JM, Pilate G, Van Doorsselaere J, Boerjan W, Jouanin L (2001) NMR evidence for benzodioxane

structures resulting from incorporation of 5-hydroxyconiferyl alcohol into lignins of O-methyltransferase-deficient poplars. J Agric Food Chem 49: 86-91
Pubmed: Author and Title
CrossRef: Author and Title
Google Scholar: Author Only Title Only Author and Title

Rencoret J, Ralph J, Marques G, Gutiérrez A, Martínez AnT, del Río JC (2013) Structural characterization of lignin isolated from coconut (Cocos nucifera) coir fibers. J Agric Food Chem 61:2434-2445
Pubmed: Author and Title
CrossRef: Author and Title
Google Scholar: Author Only Title Only Author and Title

Rinaldi R, Jastrzebski R, Clough MT, Ralph J, Kennema M, Bruijnincx PCA, Weckhuysen BM (2016) Paving the way for lignin valorisation: recent advances in bioengineering, biorefining and catalysis. Angew Chem Int Edit 55: 8164-8215
Pubmed: Author and Title
CrossRef: Author and Title
Google Scholar: Author Only Title Only Author and Title

Sato Y, Takehisa H, Kamatsuki K, Minami H, Namiki N, Ikawa H, Ohyanagi H, Sugimoto K, Antonio BA, Nagamura Y (2012) RiceXPro version 3.0: expanding the informatics resource for rice transcriptome. Nucleic Acids Res 41: D1206-D1213
Pubmed: Author and Title
CrossRef: Author and Title
Google Scholar: Author Only Title Only Author and Title

Sharma DK, Ranganathan KR, Parthasarathy MR, Bhushan B, Seshadri TR (1979) Flavonolignans from Hydnocarpus wightiana. Planta Med 37: 79-83
Pubmed: Author and Title
CrossRef: Author and Title
Google Scholar: Author Only Title Only Author and Title

Shih CH, Chu H, Tang LK, Sakamoto W, Maekawa M, Chu IK, Wang M, Lo C (2008) Functional characterization of key structural genes in rice flavonoid biosynthesis. Planta 228:1043-1054
Pubmed: Author and Title
CrossRef: Author and Title
Google Scholar: Author Only Title Only Author and Title

Sibout R, Eudes A, Mouille G, Pollet B, Lapierre C, Jouanin L, Séguin A (2005) CINNAMYL ALCOHOL DEHYDROGENASE-C and-D are the primary genes involved in lignin biosynthesis in the floral stem of Arabidopsis. Plant Cell 17: 2059-2076
Pubmed: Author and Title
CrossRef: Author and Title
Google Scholar: Author Only Title Only Author and Title

Suzuki S, Suzuki Y, Yamamoto N, Hattori T, Sakamoto M, Umezawa T (2009) High-throughput determination of thioglycolic acid lignin from rice. Plant Biotechnol 26: 337-340
Pubmed: Author and Title
CrossRef: Author and Title
Google Scholar: Author Only Title Only Author and Title

Tamura K, Stecher G, Peterson D, Filipski A, Kumar S (2013) MEGA6: molecular evolutionary genetics analysis version 6.0. Mol. Biol. Evol. b: 2725-2729
Pubmed: Author and Title
CrossRef: Author and Title
Google Scholar: Author Only Title Only Author and Title

Tobimatsu Y, Chen F, Nakashima J, Escamilla-Treviño LL, Jackson L, Dixon RA, Ralph J (2013) Coexistence but independent biosynthesis of catechyl and guaiacyl/syringyl lignin polymers in seed coats. Plant Cell 25: 2587-2600
Pubmed: Author and Title
CrossRef: Author and Title
Google Scholar: Author Only Title Only Author and Title

Tobimatsu Y, Davidson CL, Grabber JH, Ralph J (2011) Fluorescence-tagged monolignols: Synthesis, and application to studying in vitro lignification. Biomacromolecules 12: 1752-1761.
Pubmed: Author and Title
CrossRef: Author and Title
Google Scholar: Author Only Title Only Author and Title

Tobimatsu Y, Takano T, Kamitakahara H, Nakatsubo F (2008) Studies on the dehydrogenative polymerizations of monolignol ß-glycosides. Part 3: Horseradish peroxidase-catalyzed polymerizations of triandrin and isosyringin. J Wood Chem Technol 28: 69-83
Pubmed: Author and Title
CrossRef: Author and Title
Google Scholar: Author Only Title Only Author and Title

Umezawa T (2010) The cinnamate/monolignol pathway. Phytochem Rev 9: 1-17
Pubmed: Author and Title
CrossRef: Author and Title
Google Scholar: Author Only Title Only Author and Title

Updegraff DM (1969) Semimicro determination of cellulose inbiological materials Analytical Biochemistry 320: 420-424
Pubmed: Author and Title
CrossRef: Author and Title
Google Scholar: Author Only Title Only Author and Title

Vanholme R, Ralph J, Akiyama T, Lu F, Rencoret Pazo J, Christensen J, Rohde A, Morreel K, DeRycke R, Kim H, Christensen JH, Van Reusel B, Storme V, De Rycke R, Rohde A, Morreel K, Boerjan W (2010) Engineering traditional monolignols out of lignins by concomitant up-regulation F5H1 and down-regulation of COMT in Arabidopsis. Plant J 64: 885-897
Pubmed: Author and Title
CrossRef: Author and Title
Google Scholar: Author Only Title Only Author and Title

Vanholme R, Storme V, Vanholme B, Sundin L, Christensen JH, Goeminne G, Halpin C, Rohde A, Morreel K, Boerjan W (2012) A systems biology view of responses to lignin biosynthesis perturbations in Arabidopsis. Plant Cell 24: 3506-3529
Pubmed: Author and Title
CrossRef: Author and Title
Google Scholar: Author Only Title Only Author and Title

Vogt T (2010) Phenylpropanoid biosynthesis. Mol Plant 3: 2-20
Pubmed: Author and Title
CrossRef: Author and Title
Google Scholar: Author Only Title Only Author and Title

Wagner A, Tobimatsu Y, Goeminne G, Phillips L, Flint H, Steward D, Torr K, Donaldson L, Boerjan W, Ralph J (2013) Suppression of CCR impacts metabolite profile and cell wall composition in Pinus radiata tracheary elements. Plant Mol Biol 81: 105-117
Pubmed: Author and Title
CrossRef: Author and Title
Google Scholar: Author Only Title Only Author and Title

Wagner A, Tobimatsu Y, Phillips L, Flint H, Torr K, Donaldson L, Pears L, Ralph J (2011) CCoAOMT suppression modifies lignin composition in Pinus radiata. Plant J 67: 119-129
Pubmed: Author and Title
CrossRef: Author and Title
Google Scholar: Author Only Title Only Author and Title

Wang K, Zhang H, Shen L, Du Q, Li J (2010) Rapid separation and characterization of active flavonolignans of Silybum marianum by ultra-performance liquid chromatography coupled with electrospray tandem mass spectrometry. J Pharm Biomed Anal 53: 1053-1057
Pubmed: Author and Title
CrossRef: Author and Title
Google Scholar: Author Only Title Only Author and Title

Wen J-L, Sun S-L, Xue B-L, Sun R-C (2013) Quantitative structural characterization of the lignins from the stem and pith of bamboo (Phyllostachys pubescens). Holzforschung 67: 613-627
Pubmed: Author and Title
CrossRef: Author and Title
Google Scholar: Author Only Title Only Author and Title

Weng J-K, Mo H, Chapple C (2010) Over-expression of F5H in COMT-deficient Arabidopsis leads to enrichment of an unusual lignin and disruption of pollen wall formation. Plant J 64: 898-911
Pubmed: Author and Title
CrossRef: Author and Title
Google Scholar: Author Only Title Only Author and Title

Yamamura M, Hattori T, Suzuki S, Shibata D, Umezawa T (2012) Microscale thioacidolysis method for the rapid analysis of ß-O-4 substructures in lignin. Plant Biotechnol 29: 419-423
Pubmed: Author and Title
CrossRef: Author and Title
Google Scholar: Author Only Title Only Author and Title

Yamamura M, Wada S, Sakakibara N, Nakatsubo T, Suzuki S, Hattori T, Takeda M, Sakurai N, Suzuki H, Shibata D, Umezawa T (2011) Occurrence of guaiacyl/p-hydroxyphenyl lignin in Arabidopsis thaliana T87 cells. Plant biotechnol 28: 1-8
Pubmed: Author and Title
CrossRef: Author and Title
Google Scholar: Author Only Title Only Author and Title

Yang Z, Nakabayashi R, Okazaki Y, Mori T, Takamatsu S, Kitanaka S, Kikuchi J, Saito K (2013) Toward better annotation in plant metabolomics: isolation and structure elucidation of 36 specialized metabolites from Oryza sativa (rice) by using MS/MS and NMR analyses. Metabolomics 10: 543-555
Pubmed: Author and Title
CrossRef: Author and Title
Google Scholar: Author Only Title Only Author and Title

Yue F, Lu F, Sun R-C, Ralph J (2012) Syntheses of lignin-derived thioacidolysis monomers and their uses as quantitation standards. J Agric Food Chem 60: 922-928
Pubmed: Author and Title
CrossRef: Author and Title
Google Scholar: Author Only Title Only Author and Title

Zhang K, Qian Q, Huang Z, Wang Y, Li M, Hong L, Zeng D, Gu M, Chu C, Cheng Z (2006) GOLD HULL AND INTERNODE2 encodes a primarily multifunctional cinnamyl-alcohol dehydrogenase in rice. Plant Physiol 140: 972-983
Pubmed: Author and Title
CrossRef: Author and Title
Google Scholar: Author Only Title Only Author and Title

Zhao Q, Tobimatsu Y, Zhou R, Pattathil S, Gallego-Giraldo L, Fu C, Jackson LA, Hahn MG, Kim H, Chen F, Ralph J, Dixon RA (2013) Loss of function of cinnamyl alcohol dehydrogenase 1 leads to unconventional lignin and a temperature-sensitive growth defect in Medicago truncatula. Proc Natl Acad of Sci 110: 13660-13665

Pubmed: Author and Title
CrossRef: Author and Title
Google Scholar: Author Only Title Only Author and Title

Zhou J-M, Ibrahim RK (2010) Tricin—a potential multifunctional nutraceutical. Phytochemistry Rev 9: 413-424

Pubmed: Author and Title
CrossRef: Author and Title
Google Scholar: Author Only Title Only Author and Title

Zuk M, Dzialo M, Richter D, Dyminska L, Matula J, Kotecki A, Hanuza J, Szopa J (2016) Chalcone Synthase (CHS) gene suppression in flax leads to changes in wall synthesis and sensing genes, cell wall chemistry and stem morphology parameters. Front Plant Sci 7: 894

Pubmed: Author and Title
CrossRef: Author and Title
Google Scholar: Author Only Title Only Author and Title